Coupled eco-hydrology and biogeochemistry algorithms enable simulation of water table depth effects on boreal peatland net CO_2 exchange

Mohammad Mezbahuddin*[1,2], Robert F. Grant[2], and Lawrence B. Flanagan[3]

[1]*Environmental Stewardship Branch, Alberta Agriculture and Forestry, Edmonton, AB, Canada*

[2]*Department of Renewable Resources, University of Alberta, Edmonton, AB, Canada*

[3]*Department of Biological Sciences, University of Lethbridge, AB, Canada*

*corresponding author. Email addresses: symon.mezbahuddin@gov.ab.ca, mezbahud@ualberta.ca.

Abstract

Water table depth (WTD) effects on net ecosystem CO_2 exchange of boreal peatlands are largely mediated by hydrological effects on peat biogeochemistry, and eco-physiology of peatland vegetation. Lack of representation of these effects in carbon models currently limits our predictive capacity for changes in boreal peatland carbon deposits under potential future drier and warmer climates. We examined whether a process-based ecosystem model *ecosys* could simulate net ecosystem CO_2 exchange of a Western Canadian boreal fen peatland over a gradually deepening water table due to drier weather from 2004 to 2009. The goal was to test whether a process-level coupling of a prognostic WTD with 1) oxygen transport which controls energy yields from microbial and root oxidation-reduction reactions, and 2) vascular and non-vascular plant water relations could explain mechanisms that control variations in net CO_2 exchange of a boreal fen under contrasting WTD conditions i.e. shallow vs. deep WTD. A May-October WTD drawdown of ~0.25 m hastened oxygen transport to microbial and root surfaces, enabling greater microbial and root energy yields, and peat and litter decomposition, which raised modelled ecosystem respiration (R_e) by ~0.26 μmol CO_2 m^{-2} s^{-1} per 0.1 m of WTD drawdown. It also augmented nutrient mineralization, and hence root nutrient availability and uptake, which resulted in improved leaf nutrient (nitrogen) status that facilitated carboxylation, and raised modelled vascular gross primary productivity (GPP) and plant growth. The increase in modelled vascular GPP exceeded declines in modelled non-vascular (moss) GPP due to greater shading from increased vascular plant growth, and moss drying from near surface peat desiccation, thereby causing a net increase in modelled growing season GPP by ~0.39 μmol CO_2 m^{-2} s^{-1} per 0.1 m of WTD drawdown. Similar increases in GPP and R_e left no significant WTD effects on modelled seasonal and interannual variations in net ecosystem productivity (NEP).

These modelled trends were corroborated well by eddy covariance measured hourly net CO_2 fluxes (modelled vs. measured: R^2~0.8, slopes~1±0.1, intercepts~0.05 μmol m^{-2} s^{-1}), hourly measured automated chamber net CO_2 fluxes (modelled vs. measured: R^2~0.7, slopes~1±0.1, intercepts~0.4 μmol m^{-2} s^{-1}), and other biometric and laboratory measurements. Modelled drainage as an analog for WTD drawdown induced by climate change driven drying showed that this boreal peatland would switch from a large carbon sink (NEP~160 g C m^{-2} yr^{-1}) to carbon neutrality (NEP~10 g C m^{-2} yr^{-1}) should water table deepened by a further ~0.5 m. This decline in projected NEP indicated that a further WTD drawdown at this fen would eventually lead to a decline in GPP due to water limitation. Therefore, representing the effects of interactions among hydrology, biogeochemistry and plant physiological ecology on ecosystem carbon, water, and nutrient cycling in global carbon models would improve our predictive capacity for changes in boreal peatland carbon sequestration under changing climates.

1. Introduction

Northern boreal peatlands have been accumulating carbon (C) at a rate of about 20-30 g m^{-2} yr^{-1} over several thousand years (Gorham, 1991; Turunen et al., 2002). Drier and warmer future climates can affect the resilience of long-term boreal peatland C stocks by lowering water table (WT) that can halt or even reverse the C accumulation in boreal peatlands (Limpens et al., 2008; Dise, 2009; Frolking et al., 2011). To maintain and protect the C sequestration potentials of boreal peatlands we need an improved predictive capacity of how these C stocks would behave under future drier and warmer climates. However, boreal peatland C processes are currently under-represented in global C models largely due to inadequate simulation of hydrologic feedbacks to C cycles (St-Hilaire et al., 2010; Sulman et al., 2012). This can be overcome by integrating interactions between eco-hydrology of peatland vegetation, and peat biogeochemistry into finer resolution process models that can eventually be scaled up into larger spatial and temporal scale C models (Waddington et al., 2015).

The hydrologic feedbacks to boreal peatland C processes are largely mediated by water table depth (WTD) variation and its effects on peat-microbe-plant-atmosphere exchanges of C, energy, water and nutrients (Grant et al., 2012). WTD drawdown can affect net ecosystem productivity (NEP) of boreal peatlands through its effects on ecosystem respiration (R_e) and gross primary productivity (GPP). Receding WT can cause peat pore drainage that enhances microbial O_2 availability, energy yields, growth and decomposition and hence increases R_e (Sulman et al., 2009, 2010; Cai et al., 2010; Flanagan and Syed, 2011; Peichl et al., 2014). The rate of increase in R_e due to the WTD drawdown may vary with peat moisture retention and quality of peat forming substrates (Preston et al., 2012). For instance, peats with low moisture retention exhibit more rapid pore drainage than those with high moisture retention thus causing

more increase in R_e for similar WTD drawdowns (Parmentier et al., 2009; Sulman et al., 2009, 2010; Cai et al., 2010). Peats formed from *Sphagnum* mosses degrade at rates slower than those formed from remains of vascular plants (Moore and Basiliko, 2006). So for similar WTD drawdowns, moss peats would generate less increase in microbial decomposition and hence R_e than would sedge, reed or woody peats (Updegraff et al., 1995). Continued WTD drawdown can also cause near surface peat desiccation from inadequate recharge through capillary rise from deeper WT. Desiccation of near surface or shallow peat layers can cause a reduction in microbial decomposition that can partially or fully offset the increased decomposition in the deeper peat layers thereby yielding indistinct net effects of WTD drawdown on R_e (Dimitrov et al., 2010a).

The interactions between WTD and GPP vary across peatlands depending upon peat forming vegetation. For instance, increased aeration due to WTD drawdown enhances root O_2 availability and growth in vascular plants (Lieffers and Rothwell, 1987; Murphy et al., 2009). Enhanced root growth is also associated with greater root nutrient availability and uptake from more rapid mineralization facilitated by greater microbial energy yields, growth and decomposition under deeper WT (Choi et al., 2007). Greater root nutrient uptake in turns increases the rate of vascular CO_2 fixation and hence GPP (Sulman et al., 2009, 2010; Cai et al., 2010; Flanagan and Syed, 2011; Peichl et al., 2014). WTD drawdown, however, does not affect the non-vascular (e.g., moss) GPP in the same way it does the vascular GPP (Lafleur et al., 2005). Non-vascular plants mostly depend upon the water available for uptake in the near surface or shallow peat layers (Dimitrov et al., 2011). These layers can drain quickly with receding WT and thus have to depend on moisture supply through capillary rise from deeper WT (Dimitrov et al., 2011; Peichl et al., 2014). If recharge through the capillary rise is not adequate, near surface peat desiccation occurs which slows moss water uptake, causes eventual drying of mosses and

93 reduces moss GPP (Lafleur et al., 2005; Riutta 2008; Sonnentag et al., 2010; Sulman et al., 2010;
94 Dimitrov et al., 2011; Kuiper et al., 2014; Peichl et al., 2014). Near surface peat desiccation also
95 suppresses vascular root water uptake from the desiccated layers (Lafleur et al., 2005; Dimitrov
96 et al., 2011). But enhanced root growth and elongation facilitated by improved O_2 status in the
97 newly aerated deeper peat layers under deeper WT enables vascular roots to take up water from
98 wetter deeper layers (Dimitrov et al., 2011). If deeper root water uptake offsets the reduction in
99 water uptake from desiccated near surface layers, vascular transpiration (T), canopy stomatal
100 conductance (g_c) and hence GPP are sustained under deeper WT (Dimitrov et al., 2011). But if
101 the WT falls below certain threshold level under which deeper root water uptake can no longer
102 sustain vascular T, g_c and hence vascular GPP declines (Lafleur et al., 2005; Wu et al., 2010).

103 WTD variation can thus affect boreal peatland NEP through its effects on peat moisture
104 and aeration and consequent root and microbial oxidation-reduction reactions and energy yields.
105 To predict how boreal peatlands would behave under future drier and warmer climates, a
106 peatland C model thus needs to simulate WTD dynamics that determine the boundary between
107 aerobic and anaerobic zones and controls peat biogeochemistry. However, most of the current
108 process-based peatland C models either do not simulate a continuous anaerobic zone below a
109 prognostic WT (e.g., Baker et al., 2008; Schaefer et al., 2008; Tian et al., 2010), or do not
110 simulate peat saturation since any water in excess of field capacity is drained in those models
111 (e.g., Gerten et al., 2004; Krinner et al., 2005; Weng and Luo, 2008). Moreover, instead of
112 explicitly simulating the above-described hydrological and biological interactions between peat
113 aeration and biogeochemistry, most of those models use scalar functions of soil moisture
114 contents to inhibit R_e and GPP under low or high moisture conditions (e.g., Frolking et al., 2002;
115 Zhang et al., 2002; Bond-Lamberty et al., 2007; St-Hilaire et al., 2010; Sulman et al., 2012).

Consequently, those peatland C models could not simulate declines in GPP and R_e due to shallow WT while simulating WTD effects on CO_2 exchange of peatlands across northern US and Canada (Sulman et al., 2012). Furthermore, the approach of using scalar functions to simulate moisture limitations to GPP and R_e requires site-specific parameterization of model algorithms which reduces scalabitiy of those peatland C models.

1.1. Objective and rationale

In this study, we tested a process-based terrestrial ecosystem model *ecosys* against eddy covariance (EC) net CO_2 fluxes measured over a drying period from 2004 to 2009 in a western Canadian boreal fen peatland in Alberta, Canada (will be termed as WPL hereafter) (Syed et al., 2006; Flanagan and Syed, 2011). The objective was to test whether the coupling of a dynamic WTD that arises from vertical and lateral water fluxes as a function of a soil moisture retention scheme with 1) oxygen transport, 2) microbial and root oxidation-reduction reactions and energy yields, and 3) root, microbial and plant growth and uptake within a soil-plant-microbe-atmosphere water, C and nutrient (nitrogen, phosphorus) scheme in an ecosystem process model could explain underlying processes that govern hydrological effects on net CO_2 exchange of a northern boreal fen under contrasting WTD conditions (e.g., shallower vs. deeper WTD). This study would reconcile our knowledge on the feedback mechanisms among hydrology, eco-physiology, and biogeochemistry of peatlands which are predominantly based upon inferences drawn from EC-gap filled values that include empirically modelled estimates. It would also provide us with a better instight and improved predictive capacity on how carbon deposits in northern boreal peatlands would behave under changing climates. Rigorous site-scale testing of coupled eco-hydrology and biogeochemistry algorithms in ecosystem process models such as

138 *ecosys* would provide us with important insights to improve large-scale representation of these
139 processes into next generation land surface models.

140 **1.2. Hypotheses**

141 In an eddy covariance (EC) study, Flanagan and Syed (2011) found no net effect of a
142 weather driven WTD drawdown on NEP of WPL over 2004-2009. From the regressions of EC-
143 derived GPP and R_e on site measured WTD, they inferred that the absence of a net effect on NEP
144 was caused by similar increases in GPP and R_e with WTD drawdown. We hypothesized that
145 coupled eco-hydrology and biogeochemistry algorithms in *ecosys* would be able to simulate and
146 explain underlying mechanisms of these effects of WTD drawdown on GPP and R_e and hence
147 NEP at the WPL. We tested the following four central hypotheses:

148 (1) WTD drawdown would increase R_e of the northern fen at the WPL. This effect of WTD
149 drawdown on R_e could be modelled by simulation of peat pore drainage and improved peat
150 aeration that would increase the energy yields from aerobic microbial decomposition and hence
151 would increase R_e.

152 (2) WTD drawdown would increase GPP of the northern fen at the WPL. This effect of WTD
153 drawdown on GPP could be modelled by simulating enhanced microbial activity due to WTD
154 drawdown that would cause more rapid nutrient mineralization and greater root nutrient
155 availability and uptake, greater leaf nutrient concentrations and hence increased GPP.

156 (3) Increase in R_e with WTD drawdown (hypothesis 1) would cease should WTD fall below a
157 threshold depth. This threshold WTD effect on R_e could be modelled by simulating inadequate
158 recharge of the near surface peat layers through capillary rise from the deeper WTD below the
159 threshold level that would cause desiccation of those layers. Drying of near surface peat layers

and the surface residue could reduce near surface and surface peat respiration that would partially offset the increase in deeper peat respiration due to aeration.

(4) Net effect of threshold WTD on GPP would be driven by the balance between how WTD would affect vascular vs. non-vascular GPP. This threshold WTD effect on GPP would be modelled by simulating vascular vs. non-vascular water relations under deeper WTD below the threshold level. Near surface peat desiccation in hypothesis 3 would reduce peat water potential and hydraulic conductivity and hence vascular and non-vascular water uptake from desiccated near surface layers. Since non-vascular mosses depend mainly on near surface peat layers for moisture supply, reduction in moss water uptake would cause a reduction in moss water potential and hence moss GPP. On the contrary, suppression of vascular root water uptake from desiccated near surface layers under deeper WT would be offset by increased deeper root water uptake from newly aerated deeper peat layers with higher water potentials that would sustain vascular canopy water potential (ψ_c), canopy stomatal conductance (g_c) and GPP.

2. Methods

2.1. Model development

Ecosys is a process-based terrestrial ecosystem model that simulates 3D water, energy, carbon and nutrient (nitrogen, phosphorus) cycles in different peatlands (Dimitrov et al., 2011; Grant et al., 2012; Sulman et al., 2012; Mezbahuddin et al., 2014, 2015, 2016). *Ecosys* algorithms that govern the effects of WTD variations on ecosystem net CO_2 exchange which are related to our hypotheses are described below. These algorithms in *ecosys* are derived from published independent basic research which describe eco-hydrological and biogeochemical mechanisms that govern carbon, nutrient (N, P), water, and energy balance of terrestrial ecosystems. Equations representing *ecosys* algorithms related to our hypotheses are cited within

183 the text, and are listed in the sections S1-S4 in the supplementary material with references to
184 their sources for further clarification. These site-independent basic terrestrial ecosystem process
185 algorithms in *ecosys* are thus not parameterized for each peatland site. Instead the coupled
186 algorithms are fed with peatland-specific measurable soil, weather, vegetation and management
187 inputs to simulate C, nutrient (N, P), water and energy balance of that particular peatland
188 ecosystem.

189 **2.1.1. Water table depth (WTD)**

190 The WTD in *ecosys* is calculated at the end of each time step as the depth to the top of the
191 saturated zone below which air-filled porosity is zero (Eq. D32). It is the depth at which lateral
192 water flux is in equilibrium with the difference between vertical influxes (precipitation) and
193 effluxes (evapotranspiration). Lateral water transfer between modelled grid cells in *ecosys* and
194 the adjacent ecosystem occurs to and from a set external WTD (WTD_x) over a set distance (L_t)
195 (Fig. 2). The WTD_x represents average watershed WTD with reference to average hummock
196 surface. The WTD in *ecosys* is thus not prescribed, but rather controls, and is controlled by
197 lateral and vertical surface and subsurface water fluxes (Eqs. D1-D31). More detail about how
198 peatland WTD, vertical and lateral soil water flow, and soil moisture retention are modelled in
199 *ecosys* can be found in Dimitrov et al. (2010b) and Mezbahuddin et al. (2015, 2016).

200 **2.1.2. Heterotrophic respiration and WTD**

201 WTD fluctuation in *ecosys* determines the boundary between and the extent of aerobic vs.
202 anaerobic soil zones. So WTD fluctuation affects *ecosys*'s algorithms of organic oxidation-
203 reduction transformations and microbial energy yields, which drive microbial growth, substrate
204 decomposition and uptake (Fig. 1) (Eqs. A1-A30). Organic transformations in *ecosys* occur in a
205 residue layer and in each of the user defined soil layers within five organic matter-microbe

206 complexes i.e., coarse woody litter, fine non-woody litter, animal manure, particulate organic C
207 and humus (Fig. 1). Each of the complexes has three decomposition substrates i.e., solid organic
208 C, sorbed organic C and microbial residue C; the decomposition agent i.e., microbial biomass;
209 and the decomposition product i.e., dissolved organic C (DOC) (Fig. 1). Rates of the
210 decomposition and resulting DOC production in each of the complexes is a first-order function
211 of the fraction of substrate colonized by active biomasses (M) of diverse microbial functional
212 types (MFTs). The MFTs in *ecosys* are obligate aerobes (bacteria and fungi), facultative
213 anaerobes (denitrifiers), obligate anaerobes (fermenters), heterotrophic (acetotrophic) and
214 autotrophic (hydrogenotrophic) methanogens, and aerobic and anaerobic heterotrophic
215 diazotrophs (non-symbiotic N_2 fixers) (Fig. 1) (Eqs. A1-A2, A4). Biomass (M) growth of each of
216 the MFTs (Eq. A25a) is calculated from its DOC uptake (Fig. 1) (Eq. A21). The rate of M
217 growth is driven by energy yield from growth respiration (R_g) (Eq. A20) that is calculated by
218 subtracting maintenance respiration (R_m) (Eq. A18) from heterotrophic respiration (R_h) (Eq.
219 A11). The values of R_h are driven by oxidation of DOC (Eq. A13). DOC oxidation may be
220 limited by microbial O_2 reduction (Eq. A14) driven by microbial O_2 demand (Eq. A16) and
221 constrained by O_2 diffusion calculated from aqueous O_2 concentrations in soil ($[O_{2s}]$) (Eq. A17).
222 Values of $[O_{2s}]$ are maintained by convective-dispersive transport of O_2 from the atmosphere to
223 gaseous and aqueous phases of the soil surface layer (Eq. D41), by convective-dispersive
224 transport of O_2 through gaseous and aqueous phases in adjacent soil layers (Eqs. D42, D44), and
225 by dissolution of O_2 from gaseous to aqueous phases within each soil layer (Eq. D39).
226 Shallow WTD in *ecosys* can cause lower air-filled porosity (θ_g) in the wetter peat layers
227 above the WT. Lower θ_g reduces O_2 diffusivity in the gaseous phase (D_g) (Eq. D44) and gaseous
228 O_2 transport (Eqs. D41-D42) in these layers. Peat layers below the WT have zero θ_g that prevents

gaseous O_2 transport in these layers. So, under shallow WT, [O_{2s}] relies more on O_2 transport through the slower aqueous phase (Eq. D42) which causes a decline in [O_{2s}]. Decline in [O_{2s}] slows O_2 uptake (Eq. A17) and hence R_h (Eq. A14), R_g (Eq. A20) and growth of M (Eq. A25). Lower M slows decomposition of organic C (Eqs. A1-A2) and production of DOC which further slows R_h (Eq. A13), R_g and growth of M (Fig. 1). Although some MFTs can sustain DOC oxidation by reducing alternative electron acceptors (e.g., methanogens reducing acetate or CO_2 to CH_4, and denitrifiers reducing NO_x to N_2O or N_2), lower energy yields from these reactions reduce R_g (Eq. A21), and hence M growth, organic C decomposition and subsequent DOC production (Fig. 1). Slower decomposition of organic C under low [O_{2s}] also causes slower decomposition of organic nitrogen (N) and phosphorus (P) (Eq. A7) and production of dissolved organic nitrogen (DON) and phosphorus (DOP), which causes slower uptake of microbial N and P (Eq. A22) and growth of M (Eq. A29) (Fig. 1). Slower M growth causes slower mineralization (Eq. A26), and hence lowers aqueous concentrations of NH_4^+, NO_3^- and $H_2PO_4^-$ (Fig. 1).

WTD drawdown can increase θ_g that results in greater D_g (Eq. D44) and more rapid gaseous O_2 transport. A consequent rise in [O_{2s}] increases O_2 uptake (Eq. A17) and R_h (Eq. A14), R_g (Eq. A20) and growth of M (Eq. A25). Larger M hastens decomposition of organic C (Eqs. A1-A2) and production of DOC which further hastens R_h (Eq. A13), R_g and growth of M. More rapid decomposition of organic C under adequate [O_{2s}] in this period also causes more rapid decomposition of organic N and P (Eq. A7) and production of DON and DOP, which increases uptake of microbial N and P (Eq. A22) and growth of M (Eq. A29) (Fig. 1). Rapid M growth causes rapid mineralization (Eq. A26), and hence greater aqueous concentrations of NH_4^+, NO_3^- and $H_2PO_4^-$ (Fig. 1).

When WTD recedes below a certain threshold level, capillary rise from the WT can no longer support adequate recharge of the near surface peat layers and the surface litter (Eqs. D9, D12). It causes desiccation of the residue and the near surface peat layers thereby causing a reduction in water potential (ψ_s) and an increase in aqueous microbial concentrations ([M]) in each of these layers (Eq. A15). Increased [M] caused by the peat desiccation reduces microbial access to the substrate for decomposition in each of the desiccated layers and reduces R_h (Eq. A13). Reduction in R_h is calculated in *ecosys* from competitive inhibition of microbial exo-enzymes with increasing concentrations (Eq. A4) (Lizama and Suzuki, 1991).

2.1.3. WTD effects on vascular gross primary productivity

Ecosys simulates effects of WTD variation on vascular GPP from WTD variation effects on root O_2 and nutrient availability and root growth and uptake. Root O_2 and nutrient uptake in *ecosys* are coupled with a hydraulically driven soil-plant-atmosphere water scheme. Root growth in each vascular plant population in *ecosys* is calculated from its assimilation of the non-structural C product of CO_2 fixation (σ_C) (Eq. C20). Assimilation is driven by R_g (Eq. C17) remaining after subtracting R_m (Eq. C16) from autotrophic respiration (R_a) (Eq. C13) driven by oxidation of σ_C (Eq. C14). Oxidation in roots may be limited by root O_2 reduction (Eq. C14b) which is driven by root O_2 demand to sustain C oxidation and nutrient uptake (Eq. C14e), and constrained by O_2 uptake controlled by concentrations of aqueous O_2 in the soil ([O_{2s}]) and roots ([O_{2r}]) (Eq. C14d). Values of [O_{2s}] and [O_{2r}] are maintained by convective-dispersive transport of O_2 through soil gaseous and aqueous phases and root gaseous phase (aerenchyma) respectively and by dissolution of O_2 from soil and root gaseous to aqueous phases (Eqs. D39-D45). O_2 transport through root aerenchyma depends on species-specific values used for root air-filled porosity (θ_{pr}) (Eq. D45). Shallow WTD and resultant high peat moisture content in *ecosys*

274 can cause low θ_g that reduces soil O_2 transport, forcing root O_2 uptake to rely more on $[O_{2r}]$ and
275 hence on root O_2 transport determined by θ_{pr}. If this transport is inadequate, decline in $[O_{2r}]$
276 slows root O_2 uptake (Eqs. C14c-d) and hence R_a (Eq. C14b), R_g (Eq. C17) and root growth (Eq.
277 C20b) and root N and P uptake (Eqs. C23b, d, f) (Fig. 1). Root N and P uptake under shallow
278 WT is further slowed by reductions in aqueous concentrations of NH_4^+, NO_3^- and $H_2PO_4^-$ (Eqs.
279 C23a, c, e) from slower mineralization of organic N and P (Fig. 1). Slower root N and P uptake
280 reduces concentrations of non-structural N and P products of root uptake (σ_N and σ_P) with
281 respect to that of σ_C in leaves (Eq. C11), thereby slowing CO_2 fixation (Eq. C6) and GPP.
282 WTD drawdown facilitates rapid D_g which allows root O_2 demand to be almost entirely
283 met from $[O_{2s}]$ (Eqs. C14c-d) and so enables more rapid root growth and N and P uptake (Eqs.
284 C23b, d, f). Increased root growth and nutrient uptake is further stimulated by increased aqueous
285 concentrations of NH_4^+, NO_3^- and $H_2PO_4^-$ (Eqs. C23a, c, e) from more rapid mineralization of
286 organic N and P during deeper WT (Fig. 1). Greater root N and P uptake increases
287 concentrations of σ_N and σ_P with respect to σ_C in leaves (Eq. C11), thereby facilitating rapid CO_2
288 fixation (Eq. C6) and GPP. When WT falls below a certain threshold, inadequate capillary rise
289 (Eqs. A9, A12) from deeper WT causes near-surface peat desiccation that reduces soil water
290 potential (ψ_s) and raises soil hydraulic resistance (Ω_s) (Eq. B9), thereby forcing lower root water
291 uptake (U_w) from desiccated layers (Fig. 1) (Eq. B6). However, deeper rooting facilitated by
292 increased $[O_{2s}]$ under deeper WT can sustain U_w (Eq. B6) from wetter deeper peat layers with
293 higher ψ_s and lower Ω_s (Eq. B9). If U_w from the deeper wetter layers cannot offset the
294 suppression in U_w from desiccated near surface layers, the resultant net decrease in U_w causes a
295 reduction in root, canopy and turgor potentials (ψ_r, ψ_c and ψ_t) (Eq. B4) and hence g_c (Eq. B2b) in

296 *ecosys* when equilibrating U_w with transpiration (T) (Eq. B14). Lower g_c reduces CO_2 diffusion
297 into the leaves thereby reducing CO_2 fixation (Eq. C6) and GPP (Eq. C1) (Fig. 1).

298 **2.1.4. WTD effects on non-vascular gross primary productivity**

299 *Ecosys* simulates non-vascular plants (e.g., mosses) as tiny plants with no stomatal
300 regulations that grow on modelled hummock and hollow grid cells (Dimitrov et al., 2011).
301 Model input for moss population is usually larger and hence intra-specific competition for lights
302 and nutrients is greater so that individual moss plant and moss belowground growth (i.e. root like
303 structures for water and nutrient uptake) are smaller (Eq. C21b). Shallower belowground growth
304 of simulated mosses in *ecosys* means the water uptake of mosses are mostly confined to the near
305 surface peat layers. When WT deepens past a threshold level, inadequate capillary rise (Eqs. D9,
306 D12) causes near-surface peat desiccation, thereby reducing ψ_s and increasing Ω_s (Eq. B9) of
307 those layers (Fig. 1). It causes a reduction in moss canopy water potential (ψ_c) while
308 equilibrating moss evaporation with moss U_w (Eq. B6). Reduced moss ψ_c causes a reduction in
309 moss carboxylation rate (Eqs. C3, C6a) and moss GPP (Fig. 1) (Eq. C1).

310 **2.2. Modelling experiment**

311 **2.2.1. Study site**

312 The peatland eco-hydrology and biogeochemistry algorithms in *ecosys* were tested in this
313 study against measurements of WTD and ecosystem net CO_2 fluxes at a flux station of the
314 Fluxnet-Canada Research Network established at the WPL (latitude: 54.95°N, longitude:
315 112.47°W). The study site is a moderately nutrient-rich treed fen peatland within the Central
316 Mixed-wood Sub-region of Boreal Alberta, Canada. Peat depth around the flux station was about
317 2 m. This peatland is dominated by stunted trees of black spruce (*Picea mariana*) and tamarack
318 (*Larix laricina*) with an average canopy height of 3 m. High abundance of a shrub species *Betula*

319 *pumila* (dwarf birch), and the presence of a wide range of mosses e.g., *Sphagnum* spp., feather
320 moss, and brown moss characterize the under-storey vegetation of WPL. The topographic,
321 climatic, edaphic and vegetative characteristics of this site were described in more details by
322 Syed et al. (2006).

323 **2.2.2. Field data sets**

324 *Ecosys* model inputs of half hourly weather variables i.e. incoming shortwave and
325 longwave radiation, air temperature (T_a), wind speed, precipitation and relative humidity during
326 2003-2009 were measured by Syed et al. (2006) and Flanagan and Syed (2011) at the
327 micrometeorological station installed at the WPL. To test the adequacy of WTD simulation in
328 *ecosys*, modelled outputs of hourly WTD were tested against WTD measured at the WPL with
329 respect to average hummock surface by Flanagan and Syed (2011). To examine how well *ecosys*
330 simulated net ecosystem CO_2 exchange at the WPL, we tested hourly modelled net ecosystem
331 CO_2 fluxes against hourly accumulated measurements (average of two half-hourly) collected by
332 Syed et al. (2006) and Flanagan and Syed (2011) by using eddy covariance (EC) micro-
333 meteorological approach. Each of these EC-measured net CO_2 fluxes consisted of an eddy flux
334 and a storage flux (Syed et al. 2006). Erroneous flux measurements due to stable air conditions
335 were screened out with the use of a minimum friction velocity (u*) threshold of 0.15 m s^{-1} (Syed
336 et al. 2006). The net CO_2 fluxes that survived the quality control were used to derive half hourly
337 R_e (=nighttime net CO_2 fluxes) and GPP (=daytime net CO_2 fluxes – R_e) (Barr et al., 2004; Syed
338 et al., 2006). To derive daily, seasonal and annual estimates of GPP, and R_e, the data gaps
339 resulting from the quality control were filled based on empirical relationships between soil
340 temperature at a shallow depth (0.05 m) and measured half hourly R_e, and between incoming
341 shortwave radiation and measured half hourly GPP using 15-days moving windows. The gap-

342 filled R_e and GPP were then summed up for each half hour to fill NEP data gaps to derive daily,
343 seasonal and annual estimates of EC-gap filled NEP (Barr et al., 2004; Syed et al., 2006).

344 Soil CO_2 fluxes measured by automated chambers can provide a valuable supplement to
345 EC CO_2 fluxes in testing modelled respiration by providing more continuous measurements than
346 EC. So, we also tested our modelled outputs against half-hourly automated chamber
347 measurements by Cai et al. (2010) at the WPL. These CO_2 flux measurements were carried out
348 during ice-free periods (May-October) of 2005 and 2006 over both hummocks and hollows by
349 using a total of 9 non-steady state automatic transparent chambers (Cai et al., 2010). Along with
350 soil respiration these chamber CO_2 fluxes included fixation and autotrophic respiration from
351 dwarf shrubs, herbs and mosses (Cai et al., 2010).

352 **2.2.3. Model run**

353 *Ecosys* model run to simulate WTD effects on net CO_2 exchange of WPL had a
354 hummock and a hollow grid cell that exchanged water, heat, carbon and nutrients (N, P) between
355 them and with surrounding vertical and lateral boundaries (Fig. 2). The hollow grid cell had near
356 surface peat layer that was 0.3 m thinner than the hummock cell representing a hummock-hollow
357 surface difference of 0.3 m observed in the field (Long, 2008) (Fig. 2). Any depth with respect to
358 the modelled hollow surface would thus be 0.3 m shallower than the depth with respect to the
359 modelled hummock surface.

360 Peat organic and chemical properties at different depths of the WPL were represented in
361 *ecosys* by inputs from measurements either at the site (e.g., Syed et al., 2006; Flanagan and Syed,
362 2011) or at similar nearby sites (e.g., Rippy and Nelson, 2007) (Fig. 2). *Ecosys* was run for a spin
363 up period of 1961-2002 under repeating 7-year sequences of hourly weather data (shortwave and

364 longwave radiation, air temperature, wind speed, humidity and precipitation) recorded at the site
365 from 2003 to 2009. There was a drying trend observed from 2003 to 2009 due to diminishing
366 precipitation that caused WTD drawdown in the watershed in which WPL is located, which
367 lowered the WT of this fen peatland (Flanagan and Syed, 2011). To accommodate the gradual
368 drying effects of catchment hydrology on modelled fen peatland WTD, we set the WTD_x at
369 different levels based on the annual wetness of weather, e.g., shallow, intermediate, and deep
370 (WTD_x=0.19, 0.35 and 0.72 m below the hummock surface, or 0.11 m above and 0.05 and 0.42
371 m below the hollow surface) (Fig. 2). There was no exchange of water through lower model
372 boundary to represent the presence of nearly impermeable clay sediment underlying the peat
373 (Syed et al., 2006) (Fig. 2). Variations in peat surface with WTD variations, which is an
374 important hydrologic self-regulation of boreal peatlands (Dise, 2009), was not represented in this
375 version of *ecosys*.

376 At the start of the spin up run, the hummock grid cell was seeded with an evergreen
377 needle leaf and a deciduous needle leaf over-storey plant functional types (PFT) to represent the
378 black spruce and tamarack trees at the WPL. The hollow grid cell was seeded with only the
379 deciduous needle leaf over-storey PFTs since the black spruce trees at the WPL only grew on the
380 raised areas. Each of the modelled hummock and the hollow was also seeded with a deciduous
381 broadleaved vascular (to represent dwarf birch) and a non-vascular (to represent mosses) under-
382 storey PFTs. The planting densities were such that the population densities of the black spruce,
383 tamarack, dwarf birch and moss PFTs were 0.16, 0.14, 0.3, and 500 m^{-2} respectively at the end of
384 the spin up run so as to best represent field vegetation (Syed et al., 2006; Mezbahuddin et al.,
385 2016). To include wetland adaptation, we used a root porosity (θ_{pr}) value of 0.1 for the two over-
386 storey PFTs and a higher θ_{pr} value of 0.3 for the under-storey vascular PFT to represent better

wetland adaptation in the under-storey than the over-storey PFTs. These θ_{pr} values were used in calculating root O_2 transport through aerenchyma (Eq. D45) and did not change with waterlogging throughout the model run. These θ_{pr} values were representatives of root porosities measured for various northern boreal peatland plant species (Cronk and Fennessy, 2001). Non-symbiotic N_2 fixation through association of cyanobacteria and mosses are also reported for Canadian boreal forests (Markham, 2009). This was represented in *ecosys* as N_2 fixation by non-symbiotic heterotrophic diazotrophs (Eq. A27) in the moss canopy. Further details about *ecosys* model set up to represent the hydrological, physical and ecological characteristics of WPL can be found in Mezbahuddin et al. (2016).

When the modelled ecosystem attained stable values of net ecosystem CO_2 exchange at the end of the spin-up run, we continued the spin up run into a simulation run from 2003 to 2009 by using a real-time weather sequence. We tested our outputs from 2004-2009 of the simulation run against the available site measurements of WTD, net EC CO_2 fluxes and net chamber CO_2 fluxes over those years.

2.2.4. Model validation

To examine the adequacy of modelling WTD effects on canopy, root and soil CO_2 fluxes which were summed for net ecosystem CO_2 exchange at the WPL, we spatially averaged hourly net CO_2 fluxes modelled over the hummock and the hollow to represent a 50:50 hummock-hollow ratio and then regressed against hourly EC measured net ecosystem CO_2 fluxes for each year from 2004-2009 with varying WTD. Each of these hourly EC measured net ecosystem CO_2 fluxes used in these regressions is an average of two half-hourly net CO_2 fluxes measured at a friction velocity (u*) greater than 0.15 m s^{-1} that survived quality control procedure (Sec. 2.2.2). Model performance was evaluated from regression intercepts ($a \rightarrow 0$), slopes ($b \rightarrow 1$), coefficients

410 of determination ($R^2 \rightarrow 1$), and root means squares for errors (RMSE$\rightarrow$0) for each study year to
411 test whether there was any systematic divergence between the modelled and EC measured CO_2
412 fluxes.

413 Similar regressions were performed between modelled and automated chamber measured
414 net CO_2 fluxes for ice free periods (May-October) of 2005 and 2006 to further test the robustness
415 of modelled soil respiration under contrasting WTD conditions. Each of the half-hourly
416 measured chamber net CO_2 fluxes included soil respiration, and fixation and autotrophic
417 respiration from understorey vegetation (e.g., shrubs, herbs and mosses). So, we combined
418 modelled soil respiration with modelled fixation and autotrophic respiration from understorey
419 PFTs for comparison against these chamber measured net CO_2 fluxes. We also averaged net CO_2
420 flux measurements from all of the 9 chambers for each half hour to accommodate the variations
421 in those fluxes due to microtopography (e.g., hummock vs. hollow). Two half hourly averaged
422 values of net CO_2 fluxes were then averaged again to get hourly mean net chamber CO_2 fluxes
423 for comparison against modelled hourly sums of soil and understorey fluxes averaged over
424 modelled hummock and hollow. Model performance was evaluated from regression intercepts
425 ($a \rightarrow 0$), slopes ($b \rightarrow 1$), coefficients of determination ($R^2 \rightarrow 1$), and root means squares for errors
426 (RMSE$\rightarrow$0) for each of 2005 and 2006.

427 **2.2.5. Sensitivity of modelled peatland CO_2 exchange to artificial drainage**

428 Large areas of northern boreal peatlands in Canada have been drained primarily for
429 increased forest and agricultural production since plant productivity in pristine peatlands are
430 known to be constrained by shallow WTD (Choi et al., 2007). Drainage and resultant WTD
431 drawdown can affect both GPP and R_e on a short-term basis and the vegetation composition on a
432 longer time scale thereby changing overall net CO_2 exchange trajectories of a peatland. To

predict short-term effects of drainage on WTD and hence ecosystem net CO_2 exchange of WPL, we extended our simulation run into a projection run consisting two 7-yr cycles by using repeated weather sequences of 2003-2009. While doing so, we forced a stepwise drawdown in WTD_x by 1.0 and 2.0 m from that used in spin-up and simulation runs (Fig. 2) in the first (drainage cycle 1) and the second cycle (drainage cycle 2) respectively. This projection run would give us a further insight about how the northern boreal peatland of Western Canada would be affected by further WTD drawdown as a result of drier and warmer weather as well as a disturbance such as drainage. It would also provide us with a test of how sensitive the modelled C processes were to the changes in model lateral boundary condition as defined by WTD_x in *ecosys*.

3. Results

3.1. Model performance in simulating diurnal variations in ecosystem net CO_2 fluxes

Variations in precipitation can cause change in WTD and consequent variation in diurnal net CO_2 exchange across years. *Ecosys* simulated hourly EC-measured net CO_2 fluxes well over 2004-2008 with varying precipitation (Table 1a). On a year-to-year basis, regressions of hourly modelled vs. EC-measured net ecosystem CO_2 fluxes gave intercepts within 0.1 μmol m^{-2} s^{-1} of zero, and slopes within 0.1 of one, indicating minimal bias in modelled outputs during each year from 2004-2008 (Table 1a). On a growing season (May-August) basis, regressions of modelled on measured hourly net CO_2 fluxes yielded larger positive intercepts from 2004-2009 (Table 1b). The larger intercepts were predominantly caused by modelled overestimation of growing season day-time CO_2 fluxes. This overestimation was offset by modelled overestimation of night-time CO_2 fluxes during the winter thus yielding smaller intercepts from throughout-the-year regressions of modelled vs. EC measured fluxes (Tables 1a vs. b). Values for coefficients of

456 determination (R^2) were ~ 0.8 ($P < 0.001$) for all years from both throughout-the-year and
457 growing season regressions (Tables 1a, b). RMSEs were < 2.0 and ~2.5 μmol m^{-2} s^{-1} for whole
458 year regressions from 2004-2008 (Table 1a) and for growing season regressions from 2004-2009
459 (Table 1b) respectively. Much of the variations in EC measured CO_2 fluxes that was not
460 explained by the modelled fluxes could be attributed to a random error of ~20% in EC
461 methodology (Wesely and Hart, 1985). This attribution was further corroborated by root mean
462 squares for random errors (RMSRE) in EC measurements, calculated for forests with similar
463 CO_2 fluxes from Richardson et al. (2006) that were similar to RMSE (Tables 1a, b). The similar
464 values of RMSE and RMSRE also indicated that further constraint in model testing could not be
465 achieved without further precision in EC measurements.
466 Regressions of modelled vs. chamber measured net CO_2 fluxes gave R^2 of ~0.7 for ice-
467 free periods (May-October) of 2005 and 2006 indicated that the variations in soil respiration, and
468 the fixation and aboveground autotrophic respiration due to WTD drawdown were modelled well
469 (Table 1c). Smaller intercepts from those regressions meant lower model biases in simulating
470 soil and understorey CO_2 fluxes under deepening WT (Table 1c). Although the slope was within
471 0.1 of one in 2005, it was a bit smaller in 2006 indicating lower modelled vs. chamber measured
472 soil and understorey net CO_2 fluxes in 2006 (Table 1c). It was because some of the nighttime
473 chamber fluxes in warmer nights of summer 2006 were as large as the EC measured ecosystem
474 net CO_2 fluxes corresponding to those same hours which could not be modelled to their full
475 extent. RMSE lower than RMSRE meant the errors in modelling soil and understorey CO_2 fluxes
476 were within the limit of random errors due to chamber measurements (Table 1c). It further
477 indicated the robustness of modelled outputs for soil and understorey CO_2 fluxes under different
478 WTD conditions (e.g., shallower in 2005 vs. deeper in 2006) (Table 1c).

3.2. Seasonality in WTD and net ecosystem CO_2 exchange

Ecosys simulated the seasonal and interannual variations in WTD from 2004 to 2009 well at the WPL (Figs. 3b, d, f, h, j, l) (Mezbahuddin et al., 2016). Seasonality in net CO_2 exchange at the WPL was predominantly governed by that in temperature which controlled the seasonality in phenology and GPP as well as that in R_e. *Ecosys* simulated the seasonality in phenology and hence GPP, and R_e well during a gradual growing season WTD drawdown from 2004 to 2009 which was apparent by good agreements between modelled vs. EC-gap filled daily NEP (Fig. 3) and modelled vs. EC-measured hourly net CO_2 fluxes (Table 1). Modelled NEP throughout the winters of most of the years were more negative than the EC-gap filled NEP indicating larger modelled CO_2 effluxes than EC-gap filled fluxes during the winter (Fig. 3). The onset of photosynthesis at the WPL varied interannually depending upon spring temperature which was also modelled well by *ecosys*. For instance, *ecosys* modelled a smaller early growing season (May) GPP and hence NEP in 2004 with a cooler spring than 2005 which was also apparent in daily EC-gap filled NEP (Figs. 3a vs. c).

3.3. WTD effects on diurnal net ecosystem CO_2 exchange

WTD variation can affect diurnal net CO_2 exchange by affecting peat O_2 status and consequently root and microbial O_2 and nutrient availability, growth and uptake thereby influencing CO_2 fixation and respiration. *Ecosys* simulated WTD effects on diurnal net CO_2 exchange at the WPL well over three 10-day periods with comparable weather conditions (radiation and air temperature) during late growing seasons (August) of 2005, 2006 and 2008 (Fig. 4). A WTD drawdown from August 2005 to August 2006 in *ecosys* caused a reduction in peat water contents and a consequent increase in O_2 influxes from atmosphere into the peat that eventually caused an increase in modelled soil CO_2 effluxes (Fig. 5c). This stimulation of soil

502 respiration was corroborated by modelled vs. chamber measured (Cai et al., 2010) night-time soil
503 CO_2 fluxes and understorey autotrophic respiration (R_a) in August 2006 with deeper WTD which
504 were larger than those in 2005 with shallower WTD (Fig. 5b). Larger modelled soil CO_2 effluxes
505 in 2006 contributed to the larger modelled ecosystem CO_2 effluxes (R_e) that was also apparent in
506 night-time EC CO_2 fluxes in 2006 which were larger than those in 2005 (Fig. 5a).

507 Continued WTD drawdown into the late growing season of 2008 (Fig. 4c) sustained
508 improved peat oxygenation and hence larger modelled soil CO_2 effluxes (Fig. 5c). Consequently,
509 modelled night-time net ecosystem CO_2 fluxes, and soil and understorey CO_2 fluxes in 2006 and
510 in 2008 were similarly larger than those in 2005 which was corroborated well by EC measured
511 night-time fluxes during 2006 and 2008 vs. 2005 (Figs. 5a-b). Although night-time modelled and
512 EC measured net ecosystem CO_2 fluxes in 2008 were larger than those in 2005, the day-time
513 modelled and EC measured CO_2 fluxes in 2008 did not decline with respect to those in 2005
514 (Fig. 5a). Similar day-time fluxes in 2005 and 2008 despite larger night-time fluxes in 2008 than
515 in 2005 indicated a greater late growing season CO_2 fixation in 2008 with deeper WTD than in
516 2005 with shallower WTD.

517 Beside WTD, temperature variation also profoundly affected ecosystem net CO_2
518 exchange at the WPL. For a given WTD condition warmer weather caused increases in R_e at the
519 WPL (Figs. 4b-c and 5a-b). Night-time modelled, and EC and chamber measured ecosystem,
520 soil, and understorey CO_2 fluxes, in warmer nights of day 214, 220 and 222 were larger than
521 those in cooler nights of day 221, 224 and 218 in 2005, 2006 and 2008 respectively (Figs. 4b and
522 3a-b). However, for a given temperature modelled and EC-gap filled night-time ecosystem CO_2
523 fluxes, and modelled and chamber measured night-time soil and understorey CO_2 fluxes were
524 larger under deeper WT conditions in 2006 and 2008 than under shallower WT condition in 2005

(denoted by the grey arrows in Figs. 4b and 5a-b). It showed net WTD drawdown effect on R_e (separated from temperature effect) and hence on NEP.

The degree of R_e stimulation due to warming was also influenced by WTD at the WPL. The warming events in early to mid-August of 2006 and 2008, when WT was deeper than in late July of 2005, caused gradual increases in modelled, and EC and chamber measured night-time ecosystem, soil and understorey CO_2 effluxes (=R_e) (Figs. 6h, i, k, l). This R_e stimulation due to warming under deeper WT contributed to declines in modelled and EC-gap filled July-August NEP in 2006 and 2008 (Figs. 3e, i). Lack of similar stimulation in R_e with warming under shallower WT in 2005 did not yield a similarly evident stimulation of either modelled or EC or chamber measured ecosystem, soil and understorey night-time CO_2 effluxes (Figs. 6g, j vs. h, i, k, l) which resulted in the absence of decline in July-August NEP as occurred in 2006 and 2008 (Figs. 3c vs. e, i). Greater warming driven R_e stimulation under deeper WT further indicated the importance of WTD in mediating potential effects of future warmer climates on boreal peatland NEP.

3.4. Interannual variations in WTD and net ecosystem productivity

The effects of WTD drawdown on modelled and EC-gap filled diurnal net ecosystem CO_2 exchange also contributed to the effects of interannual variation in WTD on that of NEP. *Ecosys* simulated a site measured gradual drawdown of average growing season (May-August) WTD well from 2004 to 2009 (Fig. 7d) (Mezbahuddin et al., 2016). A small WTD drawdown simulated a large increase in growing season GPP from 2004 to 2005 as corroborated by similar increase in EC-derived GPP (Fig. 7b). This increase in GPP was also contributed by a larger GPP in May 2005 which was warmer than May 2004. This small WTD drawdown, however, did not raise either modelled or EC-derived growing season R_e from 2004 to 2005 (Fig. 7c). June and

548 July of 2005 was cooler than 2004 by over 2°C which caused cooler soil that reduced R_e in 2005.
549 Reduction in R_e in June-July 2005 due to cooler soil more than fully offset the increase in R_e due
550 to the small WTD drawdown and resulted in modelled and EC-derived R_e that were smaller in
551 the growing season of 2005 than in 2004 (Fig. 7c). Larger GPP and smaller R_e gave rise to
552 modelled and EC-gap filled growing season NEP estimates that were larger in 2005 than those in
553 2004 (Fig. 7a).

554 WTD drawdown from 2005 to 2006 raised both modelled and EC-derived growing
555 season GPP and R_e (Figs. 7b-c). Warmer growing season in 2006 caused warmer soil that further
556 contributed to the increase in modelled and EC-derived growing season R_e from 2005 with
557 shallower WT to 2006 with deeper WT (Figs. 5, 6 and 7c-d). An increase in growing season R_e
558 that was greater than the increase in growing season GPP caused a decline in modelled and EC-
559 derived growing season NEP from 2005 to 2006 (Fig. 7a). Continued growing season WTD
560 drawdown from 2006 to 2008 caused similar increases in modelled growing season GPP and R_e
561 and hence no significant change in modelled growing season NEP (Figs. 7a-d). With this
562 continued WTD drawdown from 2006 to 2008, however, EC-derived growing season GPP
563 increased more than EC-derived growing season R_e that resulted a larger EC-derived NEP in the
564 growing season of 2008 than in 2006 (Figs. 7a-d). A further drawdown in WTD from the
565 growing season of 2008 to that of 2009 caused reductions in both modelled and EC-derived
566 growing season GPP and R_e (Figs. 7a-d). Reductions in GPP and R_e from 2008 to 2009 was also
567 contributed by lower T_a in 2009 than in 2008 that caused cooler canopies and soil (Figs. 7b-d).
568 The reduction in EC-derived growing season GPP was larger than that in EC-derived growing
569 season R_e thereby causing a decrease in growing season EC-gap filled NEP from 2008 to 2009
570 (Figs. 7a- c). On the contrary, the reduction in modelled growing season GPP was smaller than

571 the reduction in modelled R_e that yielded an increase in modelled growing season NEP from
572 2008 to 2009 (Figs. 7a-c).

573 Modelled and EC-derived estimates of growing season GPP and R_e in 2009 were larger
574 than those in 2004 despite similar mean T_a in those years (Figs. 7a-d). It suggested that increases
575 in growing season GPP and R_e from 2004 to 2009 was a net effect of the deepening of average
576 growing season WT (Figs. 7a-d). It was further corroborated by polynomial regressions of
577 modelled growing season estimates of GPP and R_e against modelled average growing season
578 WTD, and similar regressions of EC-derived growing season GPP and R_e against site measured
579 average growing season WTD (Figs. 8a-c). These relationships showed that there were increases
580 in modelled and EC-derived growing season GPP and R_e with deepening of the growing season
581 WT from 2004 to 2008 after which further WTD drawdown in 2009 started to cause slight
582 declines in both GPP and R_e (Figs. 8b-c). Neither modelled nor EC-gap filled estimates of
583 growing season NEP yielded significant regressions when regressed against modelled and
584 measured growing season WTD respectively (Fig. 8a). It indicated that similar increases in
585 modelled and EC-derived growing season estimates of GPP and R_e with deepening of WT left no
586 net effects of WTD drawdown on either modelled or EC-derived growing season NEP (Figs. 7
587 and 8a).

588 Similar to the growing season trend, drawdown of both measured and modelled WTD
589 averaged over the ice free periods (May-October) from 2004 to 2008 generally stimulated annual
590 modelled and EC-derived GPP and R_e (Figs. 7f, g, h and 8e, f). Similar increases in both
591 modelled and EC-derived annual GPP and R_e with WTD drawdown left no net WTD effects on
592 modelled and EC-gap filled annual NEP (Figs. 7e, 8d). Although modelled WTD effects on GPP,
593 R_e and hence NEP corroborated well by EC-derived GPP, R_e and EC-gap filled NEP, the

modelled growing season and annual GPP and R_e were consistently higher than the EC-derived estimates of those throughout the study period (Figs. 7-8).

Increased GPP with WTD drawdown (Figs. 7b, f and 8b, e) was modelled predominantly through increased root growth and uptake of nutrients and consequently improved leaf nutrient status and hence more rapid CO_2 fixation in vascular PFTs. Under shallow WT during the growing season of 2004, roots in modelled black spruce and tamarack PFTs hardly grew below 0.35 m from the hummock surface. Modelled root densities of both black spruce and tamarack were higher by 2-3 orders of magnitude in the top 0.19 m of the hummock (data not shown). A WTD drawdown by ~0.4 m from the growing season of 2004 to that of 2009 caused increase in maximum modelled rooting depth in both PFTs (Table 2). Increased root growth in modelled vascular PFTs augmented root surface area for nutrient uptake under deeper WT in the growing season of 2009 than in 2004. Increased root surface area along with increased nutrient availability due to more rapid mineralization with improved aeration as a result of WTD drawdown from 2004 to 2009 caused improved root nutrient uptake in modelled vascular PFTs. Increased root growth, nutrient availability and hence uptake due to WTD drawdown from the growing season of 2004 to that of 2009 caused an increase in modelled foliar N concentrations in black spruce, tamarack and dwarf birch PFTs driving the increases in GPP modelled over this period (Figs. 7b, f and 8b, e) (Table 2).

3.5. Simulated drainage effects on WTD and NEP

Artificial drainage can drastically alter WTD in a peatland that can cause dramatic changes in peatland NEP by shifting the balance between GPP and R_e. Projected growing season WT was deeper by ~0.5 m and ~0.55 m respectively from those in the real-time simulation in drainage cycles 1 and 2 in all the years from 2004 to 2009 (Fig. 9a). Modelled growing season

GPP increased with drainage-induced WTD drawdown up to ~0.5 m below the hollow surface (~0.8 m below the hummock surface) below which GPP decreased (Figs. 9c, f). The WTD drawdown affected modelled vascular and non-vascular growing season GPP quite differently. Modelled growing season vascular GPP increased with WTD drawdown before it plateaued and eventually decreased when WTD fell below ~0.6 m from the hollow surface (~0.9 m below the hummock surface) (Figs. 10a, c, e). On the contrary, modelled non-vascular growing season GPP continued to decrease with WTD drawdown below ~0.1 m from the hollow surface (~0.4 m below the hummock surface) (Figs. 10a-b, d).

WTD drawdown due to simulated drainage not only affected modelled growing season GPP but also affected, and was affected by, the associated change in transpiration from vascular canopies. Deeper WTD_x in drainage cycle 1 caused larger hydraulic gradients and greater lateral discharge thereby deepening the WT with respect to that in the real-time simulation (Figs. 10a). Larger GPP throughout the growing seasons of 2004-2007 in the drainage cycle 1 than in the real-time simulation caused a greater vertical water loss through rapid transpiration from vascular canopies that further contributed to this deepening of WT (Fig. 9b). However, greater lateral water discharge in drainage cycle 2 caused by deeper WTD_x did not deepen the modelled growing season WT much below that in cycle 1 (Fig. 9a). The larger lateral water loss through discharge in drainage cycle 2 than in cycle 1 was mostly offset by slower vertical water losses due to vascular plant water stress as indicated by smaller GPP in the drainage cycle 2 (Fig. 9b). The changing feedbacks between WTD, and GPP and plant water relations in *ecosys* also indicated the ability of the model to simulate hydrological self-regulation which is an important characteristic of peatland eco-hydrology (Dise, 2009).

639 Modelled growing season R_e continued to increase with projected drainage driven WTD
640 drawdown (Figs. 9d, g). Reductions in modelled growing season R_e from drainage cycle 1 to 2
641 during 2006-2009 indicated R_e inhibition due to desiccation of near surface peat layers and
642 surface residues (Fig. 9d). Overall GPP increased more than R_e with drainage driven initial WTD
643 drawdown that caused a small increase in modelled growing season NEP (Figs. 9 b, e).
644 Continued drainage driven WTD drawdown, however, caused declines in GPP particularly in
645 model years of 2008 and 2009 (Figs. 9c). This decrease in GPP was also accompanied by
646 increased R_e thereby causing a decrease in NEP when WT fell below a threshold of about ~0.45
647 m from the hollow surface, particularly during the drier years (Figs. 9b-g). This projected
648 drainage effect on WTD and NEP may be transient. Long-term manipulation of WTD may
649 produce different trajectories of WTD effects on C processes and plant water relations in
650 northern boreal peatlands via vegetation adaptation and succession (Strack et al., 2006; Munir et
651 al., 2014).

652 **4. Discussion**

653 **4.1. Modelling WTD effects on northern boreal peatland NEP**

654 Hourly modelled, EC measured, and chamber measured net ecosystem, and soil and
655 understorey CO_2 fluxes, and modelled and EC-derived seasonal and annual NEP, GPP and R_e
656 estimates showed that WTD drawdown raised both GPP and R_e at the WPL (Figs. 3-8). Similar
657 increases in GPP and R_e with WTD drawdown yielded no net effect of WTD drawdown on NEP
658 at the WPL during 2004-2009 (Figs. 7-8). Four central hypotheses that outlined how coupled
659 eco-hydrology and biogeochemistry algorithms in *ecosys* would simulate and explain the
660 mechanism of these WTD effects on R_e, GPP and NEP at the boreal fen peatland under study are
661 examined in details in the following sections of 4.1.1 to 4.1.4.

4.1.1. Hypothesis 1: Increase in R_e with WTD drawdown

Shallow WTD in *ecosys* caused shallow aerobic zone above WT and thicker anaerobic zone below the WT. In the shallow aerobic zone, peat O_2 concentration [O_{2s}] was well above the Michaelis-Menten constant for O_2 reduction (K_m=0.064 g m^{-3}) and hence DOC oxidation and consequent microbial uptake and growth in *ecosys* was not much limited by [O_{2s}] (Eqs. A17a, C14c). On the contrary, [O_{2s}] in the thicker anaerobic zone below the WT was well below K_m so that DOC oxidation was coupled with DOC reduction by anaerobic heterotrophic fermenters, which yielded much less energy (4.4 kJ g^{-1} C) than did DOC oxidation coupled with O_2 reduction (37.5 kJ g^{-1} C) (Fig. 1) (Eq. A21). Lower energy yields in the thicker anaerobic zone resulted in slower microbial growth (Eq. A25) and R_h (Eq. A13). Since the anaerobic zone in *ecosys* was thicker than the aerobic zone under shallow WT, lower modelled R_h in the anaerobic zone contributed to reduced modelled soil respiration and hence R_e that was corroborated by EC and chamber measurements at the WPL (Figs. 5-8) (Tables 1 and 2).

WTD drawdown in *ecosys* caused peat pore drainage and increased θ_g thereby deepening of the aerobic zone. It raised D_g (Eq. D44) and increased O_2 influxes into the peat (Fig. 5c) (Eqs. D42-D43). Increased O_2 influxes enhanced [O_{2s}] and stimulated R_h (Eqs. A13, A20), soil respiration and hence R_e (Figs. 5-8). Rapid mineralization of DON and DOP due to improved [O_{2s}] under deeper WT also raised aqueous concentrations of NH_4^+, NO_3^- and $H_2PO_4^-$ (Eqs. C23a, c, e) that increased microbial nutrient availability, uptake (Eq. A22) and growth (Eq. A29) and further enhanced R_e (Fig. 1) (Figs. 5-8). Modelled R_e stimulation by improved peat oxygenation due to WTD drawdown was corroborated well by EC and chamber measurements at the site (Figs. 5-8) (Tables 1 and 2). However, the chamber measured nighttime net CO_2 fluxes during warmer nights of 2006 with deeper WT were sometimes as large as corresponding EC-

685 measured net ecosystem CO_2 fluxes (Figs. 5-6). Those very large chamber CO_2 effluxes could
686 not be modelled to their full extent and consequently modelled vs. chamber CO_2 flux regression
687 yielded a slope lower than 1±0.1 in 2006 (Table 1c). Although modelled rate of increase in R_e
688 with each 0.1 m of WTD drawdown was larger than EC-derived rate, it is still comparable with
689 rates reported for other similar peatlands (Table 2). Kotowska (2013) carried out chamber based
690 field measurements and laboratory incubation experiments in a moderately rich fen very close to
691 our study site which reported that a WTD drawdown driven stimulation of aerobic microbial
692 decomposition contributed to increased R_e. Mäkiranta et al. (2009) also found rapid microbial
693 decomposition in a Finish peatland due to thicker aerobic zone and consequently larger amounts
694 of decomposable organic matter exposed to aerobic oxidation.

695 Apart from WTD, peat warming in *ecosys* also increased rates of decomposition (Eq. A1)
696 through an Arrhenius function (Eq. A6) and increased R_h and R_e (Figs. 4-7). Warming effect on
697 decomposition in *ecosys* was also modified by WTD. For a similar warming, greater thermal
698 diffusivity in peat with deeper WT and consequent smaller water contents caused greater peat
699 warming (Eqs. D34, D36). It enabled larger simulation of R_e during warming periods in 2006
700 and 2008 with deeper WT than in 2005 (Figs. 4-6). Increased stimulation of peat decomposition
701 by warming under deeper WT was also modelled by Grant et al. (2012) using the same model
702 *ecosys* over a northern fen peatland at Wisconsin, USA and by Ise et al. (2008) using a land
703 surface scheme named ED-RAMS (Ecosystem Demography Model version 2 integrated with the
704 Regional Atmospheric Modeling System) coupled with a soil biogeochemical model across
705 several shallow and deep peat deposits in Manitoba, Canada.

706 **4.1.2. Hypothesis 2: Increase in GPP with WTD drawdown**

707 Modelled WTD variations influenced GPP by controlling root and microbial O_2
708 availability, energy yields, root and microbial growth and decomposition, rates of mineralization
709 and hence root nutrient availability and uptake (Fig. 1). Wet soils under shallow WT caused low
710 O_2 diffusion (Fig. 5c) (Eqs. D42-D44) into the peat and consequent low $[O_{2s}]$ meant that root O_2
711 demand had to be mostly met by $[O_{2r}]$. *Ecosys* inputs for root porosity ($\theta_{pr} = 0.1$) that governed
712 O_2 transport through aerenchyma (Eq. D45) and hence maintained $[O_{2r}]$ was not enough to meet
713 the root O_2 demand in saturated soil by the two over-storey tree PFTs i.e. black spruce and
714 tamarack, causing shallow root systems to be simulated in these two tree PFTs under shallow
715 WTD (Sec. 3.4). The under-storey shrub PFT (dwarf birch) had a higher root porosity (θ_{pr}=0.3)
716 and hence had deeper rooting under shallow WT than the two tree PFTs (Sec. 3.4). Shallow
717 rooting in the tree PFTs reduced root surface area for nutrient uptake. Root nutrient uptake (Eqs.
718 C23b, d, f) in all the PFTs was also constrained by low nutrient availability due to smaller
719 aqueous concentrations of NH_4^+, NO_3^- and/or $H_2PO_4^-$ (Eqs. C23a, c, e) resulting from slower
720 mineralization (Eq. A26) of DON and DOP (Eq. A7) because of low $[O_{2s}]$ in the wet soils under
721 shallow WT (Fig. 1). Slower root growth and nutrient uptake caused lower foliar σ_N and/or σ_P
722 with respect to foliar σ_C (Eq. C11) that slowed the rates of carboxylation (Eq. C6) and hence
723 reduced vascular GPP (Eq. C1) under shallow WT.

724 WTD drawdown enhanced O_2 diffusion (Fig. 5c) (Eqs. D42-D44) and raised $[O_{2s}]$ so that
725 root O_2 demand in all the three vascular PFTs was almost entirely met by $[O_{2s}]$. Consequently
726 roots in all the PFTs could grow deeper which increased the root surface for nutrient uptake
727 (Table 2) (Sec. 3.4). Increase in modelled rooting depth due to WTD drawdown was
728 corroborated well by studies on same PFTs as in our study grown on similar peatlands very close

729 to the study site (Table 2). Murphy et al. (2009) found a significant increase in tree fine root
730 production with WTD drawdown from ~0.1 to ~0.25 m during a WTD manipulation study in a
731 Finish peatland. Beside improved root growth, greater [O_{2s}] under deeper WT also enhanced
732 rates of mineralization (Eq. A26) of DON and DOP (Eq. A7) that raised aqueous concentrations
733 of NH_4^+, NO_3^- and/or $H_2PO_4^-$ and hence facilitated root nutrient availability and uptake (Fig. 1).
734 Enhanced root nutrient uptake increased foliar σ_N and/or σ_P with respect to foliar σ_C (Eq. C11)
735 that hastened the rates of carboxylation (Eq. C6) and hence raised vascular GPP (Eq. C1) under
736 deeper WT.

737 The three modelled vascular PFT were predominantly N limited as indicated by mass-
738 based modelled foliar N to P ratios that matched well with site-measured mass-based foliar N to
739 P ratios (Table 2). Mass-based modelled and measured foliar N to P ratio in all the PFTs were
740 less than 16:1 indicating that the vegetation at the WPL was N limited (Aerts and Chapin III,
741 1999). Since the modelled PFTs were predominantly N limited, increases in foliar N
742 concentrations as a result of improved root nutrient availability, growth and nutrient uptake with
743 WTD drawdown enhanced modelled carboxylation rates and hence modelled GPP. In a similar
744 fen peatland close to our study site, Choi et al. (2007) found an increase in peat NO_3^--N due to
745 enhanced mineralization and nitrification stimulated by a WTD drawdown which improved
746 foliar N status, and hence increased radial tree growth of black spruce and tamarack (Table 2).
747 Macdonald and Lieffers (1990) also found improved foliar N concentrations in black spruce and
748 tamarack trees that enhanced net photosynthetic C assimilation rates by those tree species in a
749 northern Alberta moderately rich fen (Table 2). The rates of increases in foliar N concentrations
750 in black spruce and tamarack trees due to WTD drawdown as reported in those studies are
751 comparable with those in our modelled outputs (Table 2). Although modelled rate of increase in

GPP with each 0.1 m of WTD drawdown was larger than EC-derived rate, it is still comparable with rates reported for other similar peatlands (Table 2).

4.1.3. Hypothesis 3: Microbial water stress on R_e due to WT deepening below a threshold WTD

When modelled WTD fell below a threshold of ~0.3 m from the hollow surface (~0.6 m below the hummock surface), desiccation of the surface residue layer and near surface shallow peat layers reduced microbial access to substrate for decomposition (Eq. A15) which enabled simulation of reduced R_h in those layers. When reduction in surface residue and near-surface R_h more than fully offset the increase in deeper R_h, net ecosystem R_h decreased. The offsetting effect on R_h partly contributed to simulated decrease in growing season R_e ($=R_h+R_a$) from 2008 to 2009 with WTD drawdown that was corroborated by a similar decrease in EC-derived R_e (Fig. 7c). Greater reductions in R_h in desiccated surface residue and near surface peat layers also caused the reductions in growing season R_e in drainage cycle 2 from those in cycle 1 during 2007-2009 in the simulated drainage study (Fig. 9d). Similar to our study, Peichl et al. (2014) found reductions in R_e when WTD fell below a threshold of ~0.3 m from the peat surface in a Swedish fen which could be partially attributed to reduction in near surface R_h due to desiccation. Mettrop et al. (2014) in a controlled incubation experiment found that the rates of microbial respiration in a nutrient rich Dutch fen initially increased with peat drying and consequent improved aeration. But excessive drying and consequent peat desiccation in their study reduced microbial respiration efficiency, growth and biomass. Dimitrov et al. (2010a) while modelling CO_2 exchange of a northern temperate bog using *ecosys* showed that a decrease in desiccated near surface peat respiration partially offset increased deeper peat respiration when WT deepened below a threshold of ~0.6-0.7 m from the hummock surface.

4.1.4. Hypothesis 4: Plant water stress on GPP due to WT deepening below a threshold WTD

Modelled WTD drawdown below a threshold level also caused rapid peat pore drainage and low moisture contents in the near surface peat layers which were colonized by most of the vascular root systems and all of the belowground biomasses of non-vascular mosses (Eqs. D9-D29). When WTD fell below ~0.1 m from the hollow surface (~0.4 m below the hummock surface), vertical recharge through capillary rise from the WT was not adequate to maintain near surface peat moisture. It reduced peat water potential (ψ_s) and raised peat hydraulic resistance (Ω_s) (Eq. B9) that supressed root and moss water uptake (U_w) (Eq. B6) from desiccated near surface peat layers (Fig. 1). Since moss U_w entirely depended upon moisture supply from the near surface layers, reduction in U_w from desiccation of these layers caused reduction in moss canopy water potential (ψ_c) and hence moss GPP (Fig. 1) (Eqs. C1, C4) (Mezbahuddin et al., 2016). Reduction in root U_w from desiccated near surface layers, however, was offset by increased root U_w (Eq. B6) from deeper wetter layers, which had higher ψ_s and lower Ω_s, due to deeper root growth facilitated by enhanced aeration. It enabled the vascular PFTs in *ecosys* to sustain ψ_c, canopy turgor potential (ψ_t) (Eq. B4), stomatal conductance (g_c) (Eqs. B2, C4) and hence to sustain increased GPP (Eq. C1) due to higher root nutrient availability and uptake (Fig. 1) (Mezbahuddin et al., 2016). Increased vascular GPP and consequent greater vascular plant growth further imposed limitations of water, nutrient and light to the modelled non-vascular PFTs due to interspecific competition and greater shading from the overstorey vascular PFTs. However, increases in vascular GPP due to enhanced plant nutrient status more than fully offset the suppression in moss GPP due to moss drying, and greater shading and competition from the overstorey, thereby causing a net increase in modelled GPP with WTD drawdown (Figs. 7b and

798 10b-c). This simulation of increased vascular dominance over moss with deepening of WT was
799 corroborated by several WTD manipulation studies (e.g., Moore et al., 2006, Munir et al., 2014)
800 in similar peatlands in Alberta that reported increased tree, shrub and herb growths over mosses
801 with WTD drawdown. However, increase in projected vascular GPP eventually plateaued and it
802 started to decline when WT fell below ~0.6 m from the hollow surface (~0.9 m below the
803 hummock surface) (Figs. 10c, e). It was because deeper root U_w (Eq. B6) could no longer offset
804 suppression of near-surface root U_w when WT fell below threshold WTD, thereby causing lower
805 ψ_c, ψ_t (Eq. B4), g_c (Eqs. B2, C4) and slower CO_2 fixation (Eq. C6) (Fig. 1).

806 These threshold WTD effects on modelled vascular and non-vascular plant water
807 relations were validated well by testing modelled vs. site measured hourly energy fluxes (latent
808 and sensible heat) and Bowen ratios, and modelled vs. site measured daily soil moisture at
809 different depths throughout 2004-2009 as described in Mezbahuddin et al. (2016). Riutta et al.
810 (2007) measured a reduction in moss productivity due to water limitation when WTD fell below
811 ~0.15 m from the surface in a Finish fen peatland. However, they reported a sustained vascular
812 GPP during that period indicating no vascular water stress (Riutta et al., 2007). Peichl et al.
813 (2014) measured a reduction in moss GPP due to moss drying caused by insufficient moisture
814 supply through capillary rise when WTD fell below ~0.3 m from the surface in a Swedish fen.
815 Reductions in moss GPP due to decreased moss canopy water potentials were also modelled by
816 Dimitrov et al. (2011) using the same model *ecosys* when WTD fell below ~0.3 m from the
817 hummock surface of a Canadian temperate bog. They, however, found no vascular plant water
818 stress and hence no reduction in vascular GPP during that period. Similarly, Kuiper et al. (2014)
819 found reductions in moss productivity with peat drying while vascular productivity sustained in a
820 simulated drought experiment on a Danish peat.

Continued deepening of WT can also cause vascular plant water stress and hence reductions in vascular GPP as projected in our drainage simulation (Figs. 10c, e). It can also be corroborated by field measurements across various northern boreal fen peatlands in Canada and Sweden. Sonnentag et al. (2010) found a reduction in stomatal conductance (g_c) of a canopy that included tamarack and dwarf birch and a consequent decline in GPP when WT fell below ~0.4 m from the ridge surface at a fen peatland in Saskatchewan. Peichl et al. (2014) also found a reduction in vascular GPP due to plant water stress when WTD fell below ~0.3 m from the surface in a Swedish fen. The WTD threshold for reductions in vascular GPP in those two field studies were shallower than that in our modelled projection i.e. ~0.6 m from the hollow surface (~0.9 m below the hummock surface) (Figs. 10a, c, e) thereby indicating different vertical rooting patterns determined by specific interactions between hydrologic properties and rooting. Lafleur et al. (2005) and Schwärzel et al. (2006) found much deeper WTD thresholds for reductions in vascular transpiration that could negatively affect vascular GPP over a Canadian pristine bog and a German drained fen respectively. Those WTD thresholds were ~0.65 and ~0.9 m below the surface for the pristine and drained peatland respectively, further indicating the importance of root-hydrology interactions and the resultant root adaptations, growth and uptake in determining WTD effects on vascular GPP across peatlands.

4.2. Divergences between modelled and EC-derived annual GPP, R_e and NEP

Modelled seasonal and annual GPP and R_e were consistently larger than EC-derived estimates of GPP and R_e during 2004-2009 (Figs. 7b, c, f, g). Although modelled annual GPP and R_e were larger than the EC-derived estimates, modelled annual NEP were consistently lower than the EC gap-filled annual NEP (Fig. 7e). Modelled annual NEP were smaller than EC-derived estimates because modelled R_e were larger than EC-derived estimates by margins bigger

than by what modelled GPP were larger than EC-derived estimates (Figs. 7f-g). Modelled R_e were larger than EC-derived R_e estimates mainly due to the presence of gap filled night-time CO_2 fluxes (=R_e) in EC-derived estimates which were smaller than corresponding modelled values. It was apparent in negative intercepts that resulted from regressions of modelled vs. gap-filled net CO_2 fluxes (Table S1 in supplementary material). Gap filled R_e fluxes were calculated from soil temperature (T_s) at a shallow depth (0.05 m) (Sec. 2.2.2). During night-time and in the winter, peat at this shallow depth rapidly cooled down and yielded smaller night-time gap-filled CO_2 fluxes (Figs. 3, 5 and 6). On the contrary, corresponding modelled CO_2 effluxes were affected by temperatures of not only the shallow peat layers but also the deeper peat profile that were warmer than the shallower layers and thus were larger than the gap-filled fluxes (e.g., Figs. 5a, 6h-i). Like modelled CO_2 effluxes, chamber measured CO_2 effluxes in cooler nights also did not decline as rapidly as did the corresponding gap-filled CO_2 fluxes as night progressed which further indicated the likely contribution of gap-filling artifact to CO_2 effluxes that were smaller than corresponding modelled fluxes (e.g., Figs. 5b vs. a, 6j-k vs. h-i).

Systematic uncertainties embedded in EC methodology could also have contributed to EC-derived annual and growing season R_e estimates which were smaller than the modelled values (Figs. 7c, g). The major uncertainty in the EC methodology is the possible underestimation of nighttime EC CO_2 flux measurements due to poor turbulent mixing under stable air conditions (Goulden et al., 1997; Miller et al., 2004). On the contrary, modelled biological production of CO_2 by plant and microbial respiration was independent of turbulent mixing which would thus contribute to modelled R_e that were larger than EC-derived estimates.

Complete energy balance closure in the model as opposed to incomplete (~75%) energy balance closure in EC measurements would also give rise to modelled evapotranspiration and

867 GPP values that were larger than EC-derived estimates (Figs. 7b, f) (Mezbahuddin et al., 2016).
868 Modelled GPP influenced modelled R_e through root exudation and litter fall (Fig. 1). Therefore,
869 modelled GPP that were larger than EC-derived estimates would have further contributed to
870 modelled growing season and annual R_e estimates that were larger than EC-derived estimates
871 (Figs. 7c, g).

872 Modelled GPP and hence R_e can also be larger than EC-derived estimates due to
873 uncertainties in model inputs for soil organic N, N deposition, N_2 fixation and any other sources
874 of N inputs into the modelled ecosystem. In *ecosys*, plant productivity is governed by foliar N
875 status which is constrained by root N availability and uptake. Our input for organic N into each
876 modelled peat layer was measured for corresponding depth at the site (Fig. 2). To simulate N
877 deposition, background wet deposition rates of 0.5 mg ammonium-N, and 0.25 mg nitrate-N per
878 litre of precipitation that were reported for the study area were used as model inputs. However,
879 from visual field observations, it was evident that there was a significant amount of nutrient
880 inflow with the lateral water influxes into this fen peatland from the surrounding upland forests
881 which was not quantified. To mimic this lateral nutrient inflow, we doubled the background wet
882 deposition of NH_4^+ and NO_3^- as reported for the area and used these as a surrogates of lateral
883 nutrient inflow into the modelled ecosystem. *Ecosys* also included a N_2 fixing algorithm which
884 simulated symbiotic N_2 fixation in moss canopies that was reported for the boreal forests (Sec.
885 2.2.3). We tested the adequacy of these N inputs into the model by comparing modelled leaf N
886 concentrations against those measured in the field. The modelled foliar N concentrations for
887 black spruce and tamarack PFTs corroborated well against site measurements (Table 2). To
888 further examine the contribution of uncertainty due to model inputs towards the divergence
889 between modelled and EC-derived seasonal and annual GPP and R_e, we performed a sensitivity

test where we had a parallel run without doubling the background N wet deposition rates in the model, hence simulating no lateral N influx into the modelled ecosystem. Unlike the current run with lateral N inflow, the parallel run without lateral N inflow simulated GPP and R_e which were very close to the EC-derived estimates. However, the regressions between hourly modelled net CO_2 fluxes from the parallel run and EC-measured hourly net CO_2 fluxes gave slopes of ~0.8 indicating under-simulation of the EC-measured fluxes in the parallel run with no lateral N inflow.

5. Conclusions

Our modelling study showed that, when adequately coupled in algorithms of a process-based ecosystem model, the existing knowledge of peatland eco-hydrological and peat biogeochemical processes could explain underlying mechanisms that governed WTD effects on net ecosystem CO_2 exchange of a boreal fen. Testing of our hypotheses against EC-measured net CO_2 fluxes, automated chamber fluxes and other biometric measurements at the site revealed that a drier weather driven WTD drawdown at this boreal fen raised both R_e and GPP due to improved aeration that facilitated 1) microbial and root O_2 availability, energy yields, growth and decomposition which raised microbial and root respiration; and 2) rapid nitrogen mineralization, and consequently increased root nitrogen availability and uptake that improved leaf nitrogen status and hence raised carboxylation (Figs. 1, 7-8) (Table 2). Similar increases in R_e and GPP with WTD drawdown to a certain depth caused no net WTD drawdown effect on NEP (Fig. 8). Modelled drainage projection, however, showed that further WTD drawdown caused by either drainage or climate change induced drying could cause plant water stress and reduce GPP and hence NEP of this boreal fen (Figs. 9-10). This study further reconciled and mechanistically explained the WTD effects on seasonal and annual GPP, R_e and hence NEP of this boreal fen

913 which was previously speculated from EC-derived estimates. However, although modelled CO_2
914 fluxes were validated well by the EC and chamber measured net CO_2 fluxes, modelled values of
915 annual and seasonal GPP and R_e were consistently larger than the EC-derived estimates (Table 1)
916 (Figs. 7-8) (Sec. 4.2). These discrepancies between modelled and EC-derived GPP and R_e
917 estimates also raised a potential research question of whether or not to use more robust process-
918 based estimates of these peatland C balance components instead of empirically modelled EC-
919 derived estimates that might not include some of the above discussed offsetting feedbacks in
920 peatland eco-hydrology and biogeochemistry.

921 The model algorithms that were used in this study represented coupled feedbacks among
922 ecosystem processes that governed carbon, water, energy, and nutrient (N, P) cycling in a
923 terrestrial ecosystem. These feedbacks were thus not parameterized for this particular boreal fen
924 peatland site. Instead, the modelled boreal fen was simulated from peatland specific model inputs
925 for weather, soil, and vegetation properties that had physical meaning and were quantifiable at
926 the site (Fig. 2). These modelled process level interactions were also validated by corroborating
927 modelled outputs against site measurements. On the contrary, most of the current peatland C
928 models uses scalar functions to represent these feedbacks and so those model algorithms have to
929 be parameterized for each peatland site. Therefore, the modelling approach as described in this
930 study should be more robust than the scalar feedback approach while assessing WTD effects on
931 peatland C balance under contrasting peat types, climates and hydrology, or under unknown
932 future climates. These process level feedbacks are also scalable once the peatlands of interest are
933 defined within the modelled landscapes by scalable model inputs for weather; peat hydrological,
934 physical, and biological properties; and plant functional types (Sec. 2.2.3). Current global land
935 surface models either lack or have very poor representation of these feedbacks which is thus far

936 limiting our large scale predictive capacity on WTD effects on boreal peatland C stocks. This
937 modelling exercise would thus provide valuable information to improve representation of these
938 feedbacks into next generation land surface models. Therefore, the insights gained from this
939 modelling study should be a significant contribution to our understanding and apprehension of
940 how peatlands would behave with changing hydrology under future drier and warmer climates.

Code availability

The *ecosys* model codes are listed in equation forms and sufficiently described in the supplementary material. The model codes that were written in FORTRAN will also be available on request from either symon.mezbahuddin@gov.ab.ca or rgrant@ualberta.ca.

Data availability

Field data that were used to validate model outputs are available at http://fluxnet.ornl.gov/site/292.

Author contribution

M. Mezbahuddin contributed to the model code modification and development, designing modelling experiment, simulation, validation, and analyses of modelled outputs. R. F. Grant is the original developer of the model *ecosys* and also contributed into simulation design and model runs. L. B. Flanagan was site principal investigator who led the collection, and quality control of the field data that were used to validate model outputs. M. Mezbahuddin wrote the manuscript with significant contributions from R. F. Grant and L. B. Flanagan.

Acknowledgments

Computing facilities for the modelling project was provided by Compute Canada, Westgrid, and University of Alberta. Funding for the modelling project was provided by several research awards from Faculty of Graduate Studies and Research and Department of Renewable Resources of University of Alberta and a Natural Sciences and Engineering Research Council (NSERC) of Canada discovery grant. The field research was carried out as part of the Fluxnet-Canada Research Network and the Canadian Carbon Program and was funded by grants to Lawrence B. Flanagan from NSERC, Canadian Foundation for Climate and Atmospheric Sciences, and BIOCAP Canada.

964 **References**

965 Aerts, R. and Chapin III, F.: The mineral nutrition of wild plants revisited: a re-evaluation of
966 processes and patterns, Adv. Ecol. Res., 30, 1-67, doi:10.1016/S0065-2504(08)60016-1,
967 1999.

968 Baker, I. T., Prihodko, L., Denning, A. S., Goulden, M., Miller, S., and Da Rocha, H. R.:
969 Seasonal drought stress in the Amazon: reconciling models and observations, J. Geophys.
970 Res.-Biogeo., 113, G00B01, doi:10.1029/2007JG000644, 2008.

971 Ballantyne, D. M., Hribljan, J. A., Pypker, T. G., and Chimner, R. A.: Long-term water table
972 manipulations alter peatland gaseous carbon fluxes in Northern Michigan, Wetl. Ecol.
973 Manag., 22, 35-47, doi:10.1007/s11273-013-9320-8, 2014.

974 Bond-Lamberty, B., Gower, S. T., and Ahl, D. E.: Improved simulation of poorly drained forests
975 using Biome-BGC, Tree Physiol., 27, 703-715, doi:10.1093/treephys/27.5.703, 2007.

976 Cai, T., Flanagan, L. B., and Syed, K. H.: Warmer and drier conditions stimulate respiration
977 more than photosynthesis in a boreal peatland ecosystem: analysis of automatic chambers
978 and eddy covariance measurements, Plant Cell Environ., 33, 394-407, doi:10.1111/j.1365-
979 3040.2009.02089.x, 2010.

980 Campbell, G. S.: A simple method for determining unsaturated conductivity from moisture
981 retention data, Soil Sci., 117, 311-314, 1974.

982 Choi, W. J., Chang, S. X., and Bhatti, J. S.: Drainage affects tree growth and C and N dynamics
983 in a minerotrophic peatland, Ecology, 88, 443-453, doi:10.1890/0012-
984 9658(2007)88[443:DATGAC]2.0.CO;2, 2007.

985 Cronk, J. K. and Fennessy, M. S.: Wetland plants: biology and ecology, CRC press, 2001.

986 Dimitrov, D. D., Grant, R. F., Lafleur, P. M., and Humphreys, E. R.: Modeling the effects of
987 hydrology on ecosystem respiration at Mer Bleue bog, J. Geophys. Res.-Biogeo., 115,
988 G04043, doi:10.1029/2010JG001312, 2010a.

989 Dimitrov, D. D., Grant, R. F., Lafleur, P. M., and Humphreys, E. R.: Modelling subsurface
990 hydrology of Mer Bleue bog, Soil Sci. Soc. Am. J., 74, 680–694,
991 doi:10.2136/sssaj2009.0148, 2010b.

992 Dimitrov, D. D., Grant, R. F., Lafleur, P. M., and Humphreys, E. R.: Modeling the effects of
993 hydrology on gross primary productivity and net ecosystem productivity at Mer Bleue bog,
994 J. Geophys. Res.-Biogeo., 116, G04010, doi:10.1029/2010JG001586, 2011.

995 Dise, N. B: Peatland response to global change, Science, 326, 810-811,
996 doi:10.1126/science.1174268, 2009.

997 Flanagan, L. B. and Syed, K. H.: Stimulation of both photosynthesis and respiration in response
998 to warmer and drier conditions in a boreal peatland ecosystem, Glob. Change Biol., 17,
999 2271-2287, doi:10.1111/j.1365-2486.2010.02378.x, 2011.

1000 Frolking, S., Roulet, N. T., Moore, T. R., Lafleur, P. M., Bubier, J. L., and Crill, P. M.:
1001 Modelling the seasonal to annual carbon balance of Mer Bleue bog, Ontario, Canada,
1002 Global Biogeochem. Cy., 16, 1-21, doi:10.1029/2001GB001457, 2002.

1003 Gerten, D., Schaphoff, S., Haberlandt, U., Lucht, W., and Sitch, S.: Terrestrial vegetation and
1004 water balance-hydrological evaluation of a dynamic global vegetation model, J. Hydrol.,
1005 286, 249-270, doi:10.1016/j.jhydrol.2003.09.029, 2004.

1006 Gorham, E: Northern peatlands: role in the carbon cycle and probable responses to climatic
1007 warming, Ecol. Appl., 1, 182-195, doi: 10.2307/1941811, 1991.

1008 Goulden, M. L., Daube, B. C., Fan, S. M., Sutton, D. J., Bazzaz, A., Munger, J. W., and Wofsy,
1009 S. C.: Physiological responses of a black spruce forest to weather, J. Geophys. Res.-
1010 Atmos., 102, 28987-28996, doi:10.1029/97JD01111, 1997.

1011 Grant, R. F., Desai, A. R., and Sulman, B. N.: Modelling contrasting responses of wetland
1012 productivity to changes in water table depth, Biogeosciences, 9, 4215-4231,
1013 doi:10.5194/bg-9-4215-2012, 2012.

1014 Ise, T., Dunn, A. L., Wofsy, S. C., and Moorcroft, P. R.: High sensitivity of peat decomposition
1015 to climate change through water-table feedback, Nat. Geosci., 1, 763-766,
1016 doi:10.1038/ngeo331, 2008.

1017 Kotowska, A: The long-term effects of drainage on carbon cycling in a boreal fen, M.Sc. thesis,
1018 Department of Integrative Biology, University of Guelph, Ontario, Canada, 75 pp., 2013.

1019 Krinner, G., Viovy, N., de Noblet-Ducoudré, N., Ogée, J., Polcher, J., Friedlingstein, P., Ciais,
1020 P., Sitch, S., and Prentice, I. C.: A dynamic global vegetation model for studies of the
1021 coupled atmosphere-biosphere system, Global Biogeochem. Cy., 19, GB1015,
1022 doi:10.1029/2003GB002199, 2005.

1023 Kuiper, J. J., Mooij, W. M., Bragazza, L., and Robroek, B. J.: Plant functional types define
1024 magnitude of drought response in peatland CO_2 exchange, Ecology, 95, 123-131,
1025 doi:10.1890/13-0270.1, 2014.

1026 Lafleur, P. M., Hember, R. A., Admiral, S. W., and Roulet, N. T.: Annual and seasonal
1027 variability in evapotranspiration and water table at a shrub-covered bog in southern
1028 Ontario, Canada, Hydrol. Process., 19, 3533-3550, 2005, doi: 10.1002/hyp.5842.

1029 Lieffers, V. J. and Rothwell, R. L.: Rooting of peatland black spruce and tamarack in relation to
1030 depth of water table, Can. J. Botany, 65, 817-821, doi: 10.1139/b87-111, 1987.

1031 Limpens, J., Berendse, F., Blodau, C., Canadell, J. G., Freeman, C., Holden, J., Roulet, N.,
1032 Rydin, H., and Schaepman-Strub, G.: Peatlands and the carbon cycle: from local processes
1033 to global implications – a synthesis, Biogeosciences, 5, 1475–1491, doi:10.5194/bg-5-
1034 1475-2008, 2008.

1035 Lizama, H. M. and Suzuki, I.: Kinetics of sulfur and pyrite oxidation by Thiobacillus
1036 thiooxidans. Competitive inhibition by increasing concentrations of cells, Can. J.
1037 Microbiol., 37, 182-187, doi:10.1139/m91-028, 1991.

1038 Long, K. D., Flanagan, L. B., and Cai, T.: Diurnal and seasonal variation in methane emissions
1039 in a northern Canadian peatland measured by eddy covariance, Glob. Change Biol. 16,
1040 2420-2435, doi:10.1111/j.1365-2486.2009.02083.x, 2010.

1041 Long, K. D.: Methane fluxes from a northern peatland: mechanisms controlling diurnal and
1042 seasonal variation and the magnitude of aerobic methanogenesis, M.Sc. thesis, Department
1043 of Biological Sciences, University of Lethbridge, Lethbridge, AB, Canada, 100 pp., 2008.

1044 Macdonald, S. E. and Lieffers, V. J.: Photosynthesis, water relations, and foliar nitrogen of Picea
1045 mariana and Larix laricina from drained and undrained peatlands, Can. J. Forest Res., 20,
1046 995-1000, doi:10.1139/x90-133, 1990.

1047 Mäkiranta, P., Laiho, R., Fritze, H., Hytönen, J., Laine, J., and Minkkinen, K.: Indirect regulation
1048 of heterotrophic peat soil respiration by water level via microbial community structure and
1049 temperature sensitivity, Soil Biol. Biochem., 41, 695-703,
1050 doi:10.1016/j.soilbio.2009.01.004, 2009.

1051 Markham, J. H.: Variation in moss-associated nitrogen fixation in boreal forest stands, Oecologia
1052 161, 353-359, doi: 10.1007/s00442-009-1391-0, 2009.

1053 Mettrop, I. S., Cusell, C., Kooijman, A. M., and Lamers, L. P.: Nutrient and carbon dynamics in
1054 peat from rich fens and Sphagnum-fens during different gradations of drought, Soil Biol.
1055 Biochem., 68, 317-328, doi:10.1016/j.soilbio.2013.10.023, 2014.

1056 Mezbahuddin, M., Grant, R. F., and Hirano, T.: How hydrology determines seasonal and
1057 interannual variations in water table depth, surface energy exchange, and water stress in a
1058 tropical peatland: modeling versus measurements, J. Geophys. Res.-Biogeo., 120, 2132-
1059 2157, doi:10.1002/2015JG003005, 2015.

1060 Mezbahuddin, M., Grant, R. F., and Hirano, T.: Modelling effects of seasonal variation in water
1061 table depth on net ecosystem CO_2 exchange of a tropical peatland, Biogeosciences, 11,
1062 577-599, doi:10.5194/bg-11-577-2014, 2014.

1063 Mezbahuddin, M., Grant, R.F. and Flanagan, L.B.: Modeling hydrological controls on variations
1064 in peat water content, water table depth, and surface energy exchange of a boreal western
1065 Canadian fen peatland, J. Geophys. Res.-Biogeo., 121, 2216-2242,
1066 doi:10.1002/2016JG003501, 2016.

1067 Miller, S. D., Goulden, M. L., Menton, M. C., da Rocha, H. R., de Freitas, H. C., Figueira, A. M.
1068 e. S., and de Sousa, C. A. D.: Biometric and micrometeorological measurements of tropical
1069 forest carbon balance, Ecol. Appl., 14, 114–126, doi:10.1890/02-6005, 2004.

1070 Moore, T. and Basiliko, N.: Decomposition in boreal peatlands, in: Boreal peatland ecosystems,
1071 edited by: Wieder, R. K. and Vitt, D. H., Springer Science & Business Media, 125-143,
1072 2006.

1073 Munir, T. M., Xu, B., Perkins, M., and Strack, M.: Responses of carbon dioxide flux and plant
1074 biomass to water table drawdown in a treed peatland in northern Alberta: a climate change
1075 perspective, Biogeosciences, 11, 807-820, doi:10.5194/bg-11-807-2014, 2014.

1076 Murphy, M., Laiho, R., and Moore, T. R.: Effects of water table drawdown on root production
1077 and aboveground biomass in a boreal bog, Ecosystems, 12, 1268-1282,
1078 doi:10.1007/s10021-009-9283-z, 2009.

1079 Parmentier, F. J. W., Van der Molen, M. K., de Jeu, R. A. M., Hendriks, D. M. D., and Dolman,
1080 A. J.: CO_2 fluxes and evaporation on a peatland in the Netherlands appear not affected by
1081 water table fluctuations, Agr. Forest Meteorol., 149, 1201-1208,
1082 doi:10.1016/j.agrformet.2008.11.007, 2009.

1083 Peichl, M., Öquist, M., Löfvenius, M. O., Ilstedt, U., Sagerfors, J., Grelle, A., Lindroth, A., and
1084 Nilsson, M. B.: A 12-year record reveals pre-growing season temperature and water table
1085 level threshold effects on the net carbon dioxide exchange in a boreal fen, Environ. Res.
1086 Lett., 9, 055006, doi:10.1088/1748-9326/9/5/055006, 2014.

1087 Preston, M. D., Smemo, K. A., McLaughlin, J. W., and Basiliko, N.: Peatland microbial
1088 communities and decomposition processes in the James Bay Lowlands, Canada, Front.
1089 Microbiol., 3, 70, doi:10.3389/fmicb.2012.00070, 2012.

1090 Richardson, A. D., Hollinger, D. Y., Burba, G. G., Davis, K. J., Flanagan, L. B., Katul, G. G.,
1091 Munger, J. W., Ricciuto, D. M., Stoy, P. C., Suyker, A. E., Verma, S. B., and Wofsy, S. C.:
1092 A multi-site analysis of random error in tower-based measurements of carbon and energy
1093 fluxes, Agr. Forest Meteorol., 136, 1-18, doi:10.1016/j.agrformet.2006.01.007, 2006.

1094 Rippy, J. F. and Nelson, P. V.: Cation exchange capacity and base saturation variation among
1095 Alberta, Canada, moss peats, HortScience, 42, 349-352, 2007.

1096 Riutta, T., Laine, J., and Tuittila, E. S.: Sensitivity of CO_2 exchange of fen ecosystem
1097 components to water level variation, Ecosystems, 10, 718-733, doi:10.1007/s10021-007-
1098 9046-7, 2007.

1099 Riutta, T.: Fen ecosystem carbon gas dynamics in changing hydrological conditions, Diss. For.
1100 67, Department of Forest Ecology, Faculty of Agriculture and Forestry, University of
1101 Helsinki, 46pp., 2008.

1102 Schaefer, K., Collatz, G. J., Tans, P., Denning, A. S., Baker, I., Berry, J., Prihodko, L., Suits, N.,
1103 and Philpott, A.: Combined simple biosphere/Carnegie-Ames-Stanford approach terrestrial
1104 carbon cycle model, J. Geophys. Res.-Biogeo., 113, G03034, doi:10.1029/2007JG000603,
1105 2008.

1106 Schwärzel, K., Šim˚unek, J., van Genuchten, M. T., and Wessolek, G.: Measurement and
1107 modeling of soil-water dynamics and evapotranspiration of drained peatland soils, J. Plant
1108 Nutr. Soil Sci., 169, 762-774, doi:10.1002/jpln.200621992, 2006.

1109 Sonnentag, O., van der Kamp, G., Barr, A. G., and Chen, J. M.: On the relationship between
1110 water table depth and water vapour and carbon dioxide fluxes in a minerotrophic fen, Glob.
1111 Change Biol., 16, 1762–1776, doi:10.1111/j.1365-2486.2009.02032.x, 2010.

1112 St-Hilaire, F., Wu, J., Roulet, N. T., Frolking, S., Lafleur, P. M., Humphreys, E. R., and Arora,
1113 V.: McGill wetland model: evaluation of a peatland carbon simulator developed for global
1114 assessments, Biogeosciences, 7, 3517–3530, doi:10.5194/bg-7-3517- 2010, 2010.

1115 Strack, M., Waddington, J. M., Rochefort, L., and Tuittila, E. S.: Response of vegetation and net
1116 ecosystem carbon dioxide exchange at different peatland microforms following water table
1117 drawdown, J. Geophys. Res.-Biogeo., 111, G02006, doi:10.1029/2005JG000145, 2006.

1118 Sulman, B. N., Desai, A. R., Cook, B. D., Saliendra, N., and Mackay, D. S.: Contrasting carbon
1119 dioxide fluxes between a drying shrub wetland in Northern Wisconsin, USA, and nearby
1120 forests, Biogeosciences, 6, 1115-1126, doi:10.5194/bg-6-1115-2009, 2009.

1121 Sulman, B. N., Desai, A. R., Saliendra, N. Z., Lafleur, P. M., Flanagan, L. B., Sonnentag, O.,
1122 Mackay, D. S., Barr, A. G., and van der Kamp, G.: CO_2 fluxes at northern fens and bogs
1123 have opposite responses to inter-annual fluctuations in water table, Geophys. Res. Lett., 37,
1124 L19702, doi:10.1029/2010GL044018, 2010.

1125 Sulman, B. N., Desai, A. R., Schroeder, N. M., Ricciuto, D., Barr, A., Richardson, A. D.,
1126 Flanagan, L. B., Lafleur, P. M., Tian, H., Chen, G., Grant, R. F., Poulter, B., Verbeeck, H.,

Ciais, P., Ringeval, B., Baker, I. T., Schaefer, K., Luo, Y., and Weng, E.: Impact of hydrological variations on modeling of peatland CO_2 fluxes: Results from the North American Carbon Program site synthesis, J. Geophys. Res.-Biogeo., 117, G01031, doi:10.1029/2011JG001862, 2012.

Syed, K. H., Flanagan, L. B., Carlson, P. J., Glenn, A. J., and Van Gaalen, K. E.: Environmental control of net ecosystem CO_2 exchange in a treed, moderately rich fen in northern Alberta, Agr. Forest Meteorol., 140, 97-114, doi:10.1016/j.agrformet.2006.03.022, 2006.

Tian, H., Chen, G., Liu, M., Zhang, C., Sun, G., Lu, C., Xu, X., Ren, W., Pan, S., and Chappelka, A.: Model estimates of net primary productivity, evapotranspiration, and water use efficiency in the terrestrial ecosystems of the southern United States during 1895–2007, Forest Ecol. Manag., 259, 1311-1327, doi:10.1016/j.foreco.2009.10.009, 2010.

Turunen, J., Tomppo, E., Tolonen, K., and Reinikainen, A.: Estimating carbon accumulation rates of undrained mires in Finland-application to boreal and subarctic regions, The Holocene, 12, 69-80, 2002.

Updegraff, K., Pastor, J., Bridgham, S. D., and Johnston, C. A.: Environmental and substrate controls over carbon and nitrogen mineralization in northern wetlands, Ecol. Appl., 5, 151-163, doi:10.2307/1942060, 1995.

van Genuchten, M. T.: A closed-form equation for predicting the hydraulic conductivity of unsaturated soils, Soil Sci. Soc. Amer. J., 44, 892-898, doi: 10.2136/sssaj1980.03615995004400050002x, 1980.

Waddington, J. M., Morris, P. J., Kettridge, N., Granath, G., Thompson, D. K., and Moore, P. A.: Hydrological feedbacks in northern peatlands, Ecohydrology, 8, 113-127, doi:10.1002/eco.1493, 2015.

Weng, E. and Luo, Y.: Soil hydrological properties regulate grassland ecosystem responses to multifactor global change: A modeling analysis, J. Geophys. Res.-Biogeo., 113, G03003, doi:10.1029/2007JG000539, 2008.

Wesely, M. L. and Hart, R. L.: Variability of short term eddy-correlation estimates of mass exchange, in: The ForestAtmosphere Interaction, edited by: Hutchinson, B. A., Hicks, B. B., and Reidel, D., 591-612, Dordrecht, 1985.

Wu, J., Kutzbach, L., Jager, D., Wille, C., and Wilmking, M.: Evapotranspiration dynamics in a boreal peatland and its impact on the water and energy balance, J. Geophys. Res.-Biogeo., 115, G04038, doi:10.1029/2009JG001075, 2010.

Zhang, Y., Li, C., Trettin, C. C., Li, H., and Sun, G.: An integrated model of soil, hydrology, and vegetation for carbon dynamics in wetland ecosystems, Global Biogeochem. Cy., 16, 9-1-9-17, doi:10.1029/2001GB001838, 2002.

Figure captions

Fig. 1. Schematic diagram of *ecosys* algorithms representing coupled key eco-physiological and biogeochemical (aerobic and anaerobic) processes, and plant water relations of a typical boreal fen peatland ecosystem that are affected by water table depth (WTD) fluctuation. Ψ_a, Ψ_c, and Ψ_s =atmospheric, canopy and soil water potentials; Ψ_r=vascular root or non-vascular belowground water potential; r_c=canopy stomatal resistance (=1/canopy stomatal conductance (g_c)); Ω_s=soil hydraulic resistance; Ω_r=hydraulic resistance to water flow through plants; OM=organic matter; DOC, DON, DOP=dissolved organic carbon, nitrogen, and phosphorus; POC = particulate organic C; and POM = particulate organic matter

Fig. 2. Layout for *ecosys* model run to represent biological, chemical and hydrological characteristics of a Western Canadian fen peatland. Figure is not drawn to scale. D_{humm} = depth to the bottom of a layer from the hummock surface; D_{holl} = depth to the bottom of a layer from the hollow surface; TOC = total organic C (Flanagan and Syed, 2011); TN = total nitrogen (Flanagan and Syed, 2011); TP = total phosphorus (Flanagan and Syed, 2011); CEC = Cation exchange capacity (Rippy and Nelson, 2007); the value for pH was obtained from Syed et al. (2006); WTD_x = external reference water table depth representing average water table depth of the adjacent ecosystem; L_t = distance from modelled grid cells to the adjacent watershed over which lateral discharge / recharge occurs

Fig. 3. (a, c, e, g, i, k) 3-day moving averages of modelled and EC-gap filled net ecosystem productivity (NEP) (Flanagan and Syed, 2011), and **(b, d, f, h, j, l)** hourly modelled and half hourly measured water table depth (WTD) (Syed et al., 2006; Cai et al., 2010; Long et al., 2010; Flanagan and Syed, 2011) from 2004-2009 at a Western Canadian fen peatland. A positive NEP

1184 means the ecosystem is a carbon sink and a negative NEP means the ecosystem is a carbon
1185 source. A negative WTD represents a depth below hummock/hollow surface and a positive WTD
1186 represents a depth above hummock/hollow surface

1187 **Fig. 4.** Half hourly measured **(a)** incoming shortwave radiation, and **(b)** air temperature (T_a); and
1188 **(c)** hourly modelled and half hourly measured water table depth (WTD) (Syed et al., 2006; Cai et
1189 al.; 2010, Long et al.; 2010, Flanagan and Syed, 2011) during August 2005, 2006 and 2008 at a
1190 Western Canadian fen peatland. A negative WTD represents a depth below hummock/hollow
1191 surface and a positive WTD represents a depth above hummock/hollow surface. Grey arrows
1192 indicate nights with similar temperatures

1193 **Fig. 5. (a)** Half hourly EC-gap filled (Flanagan and Syed, 2011) and hourly modelled ecosystem
1194 net CO_2 fluxes, **(b)** half hourly automated chamber measured (Cai et al., 2010) and hourly
1195 modelled understorey and soil CO_2 fluxes, and **(c)** hourly modelled soil CO_2 and O_2 fluxes
1196 during August 2005, 2006 and 2008 at a Western Canadian fen peatland. No chamber CO_2 flux
1197 measurement was available for 2008. A negative flux represents an upward flux or a flux out of
1198 the ecosystem and a positive flux represents a downward flux or a flux into the ecosystem. Grey
1199 arrows indicate nights with similar temperatures (Fig. 4)

1200 **Fig. 6. (a-c)** Half hourly observed air temperature (T_a), **(d-f)** hourly modelled and half hourly
1201 observed water table depth (WTD) (Syed et al., 2006; Cai et al., 2010; Long et al., 2010;
1202 Flanagan and Syed, 2011), **(g-i)** half hourly EC-gap filled (Flanagan and Syed, 2011) and hourly
1203 modelled ecosystem net CO_2 fluxes, **(j-l)** half hourly automated chamber measured (Cai et al.,
1204 2010) and hourly modelled understorey and soil CO_2 fluxes during July-August 2005, 2006 and
1205 2008 at a Western Canadian fen peatland. No chamber CO_2 flux measurement was available for

2008. A negative flux represents an upward flux or a flux out of the ecosystem and a positive flux represents a downward flux or a flux into the ecosystem. A negative WTD represents a depth below hummock/hollow surface and a positive WTD represents a depth above hummock/hollow surface

Fig. 7. Modelled and EC-derived (Flanagan and Syed, 2011) growing season (May-August) sums of **(a)** net ecosystem productivity (NEP), **(b)** gross primary productivity (GPP), and **(c)** ecosystem respiration (R_e) during 2004-2009; **(d)** observed mean growing season air temperature (T_a) and measured and modelled average growing season water table depth (WTD) during 2004-2009; Modelled and EC-derived (Flanagan and Syed, 2011) annual sums of **(e)** NEP, **(f)** GPP, and **(g)** R_e during 2004-2008; and **(h)** observed mean annual T_a and measured and modelled average WTD during ice free periods (May-October) of 2004-2008 at a Western Canadian fen peatland. A negative WTD represents a depth below hollow surface and a positive WTD represents a depth above hollow surface. A positive NEP means the ecosystem is a carbon sink. Annual modelled vs. EC-gap filled NEP, GPP, R_e estimates for 2009 was not compared due to the lack of flux measurements from September to December in that year.

Fig. 8. Regressions (P<0.001) of growing season (May-August) sums of modelled and EC-derived (Flanagan and Syed, 2011) **(a)** net ecosystem productivity (NEP), **(b)** gross primary productivity (GPP), and **(c)** ecosystem respiration (R_e) on growing season averages of modelled and observed water table depth (WTD) during 2004-2009; and regressions (P<0.001) of annual sums of modelled and EC-derived (Flanagan and Syed, 2011) **(d)** NEP, **(e)** GPP and **(f)** R_e on average modelled and measured WTD during ice free periods (May-October) of 2004-2008 at a Western Canadian fen peatland. A negative WTD represents a depth below hollow surface and a

positive WTD represents a depth above hollow surface. A positive NEP means the ecosystem is a carbon sink

Fig. 9. (a) Observed, real-time simulated and projected drainage simulated average growing season (May-August) water table depth (WTD); EC-derived, real-time simulated and projected drainage simulated growing season sums of **(b)** net ecosystem productivity (NEP), **(c)** gross primary productivity (GPP), and **(d)** ecosystem respiration (R_e); and regressions (P<0.001) of real-time simulated and projected drainage simulated sums of **(e)** NEP, **(f)** GPP, and **(g)** R_e on real-time simulated and projected drainage simulated average growing season WTD during 2004-2009 at a Western Canadian fen peatland. A negative WTD represents a depth below hollow surface and a positive WTD represents a depth above hollow surface. A positive NEP means the ecosystem is a C sink

Fig. 10. Real-time simulated and projected drainage simulated **(a)** average growing season (May-August) water table depth (WTD), **(b)** growing season sums of non-vascular (moss) gross primary productivity (GPP), and **(c)** growing season sums of vascular GPP; and regressions (P<0.001) of real-time simulated and projected drainage simulated sums of **(d)** non-vascular GPP, and **(e)** vascular GPP on real-time simulated and projected drainage simulated average growing season WTD during 2004-2009 at a Western Canadian fen peatland. A negative WTD represents a depth below hollow surface and a positive WTD represents a depth above hollow surface

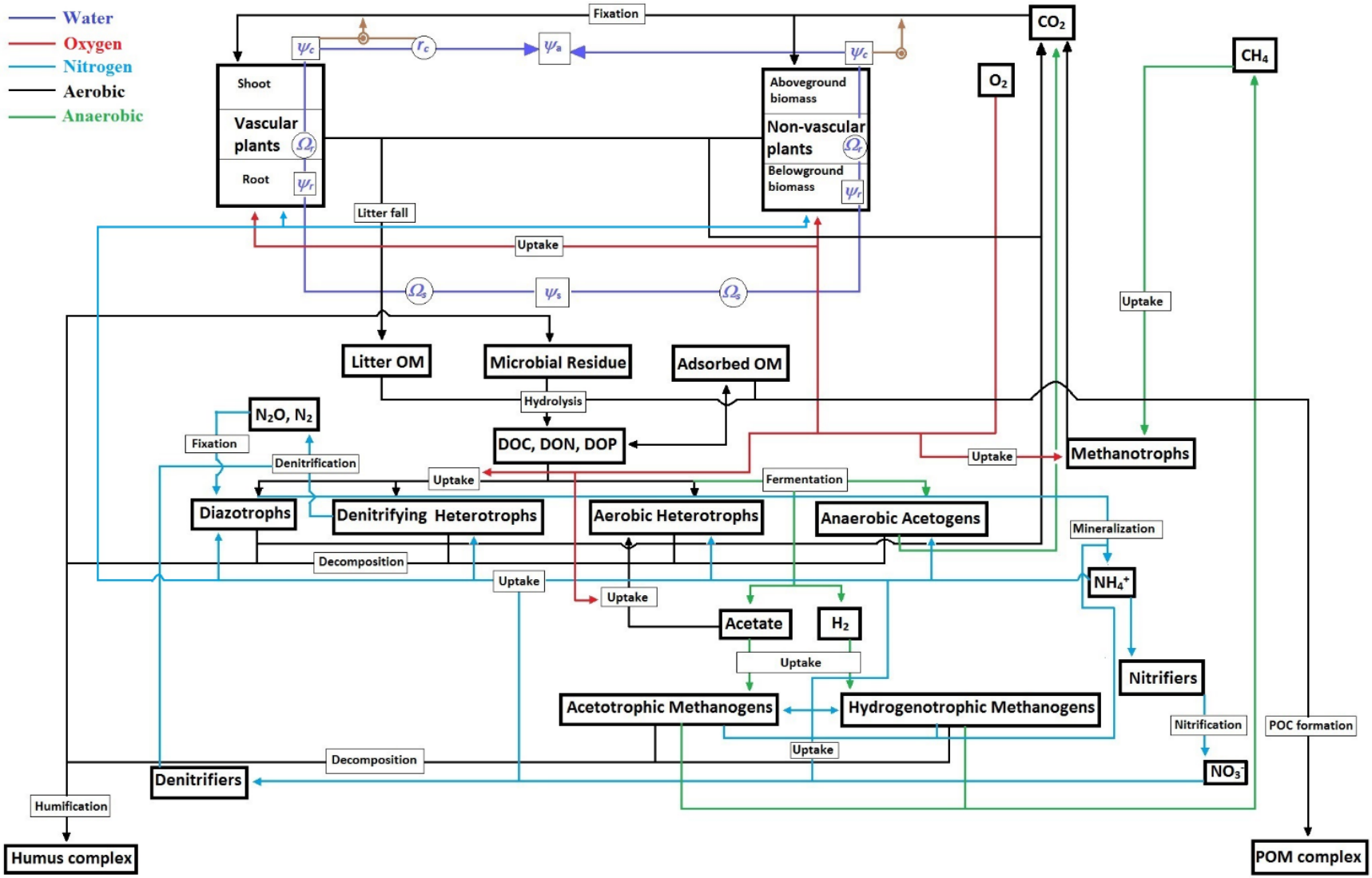

1248

1249 **Fig. 1.**

D_{humm} (m)	D_{holl} (m)	TOC (g kg^{-1})	TN (g Mg^{-1})	TP (g Mg^{-1})	pH	CEC (cmol+ kg^{-1})
0.010		463	10100	700	6.2	139
0.065						
0.085						
0.115						
0.135						
0.190						
0.295		462	13600	400		
0.305	0.005					
0.350	0.050					
0.540	0.240					
0.650	0.350					
0.720	0.420					
0.900	0.600					
1.100	0.800					
2.000	1.700					

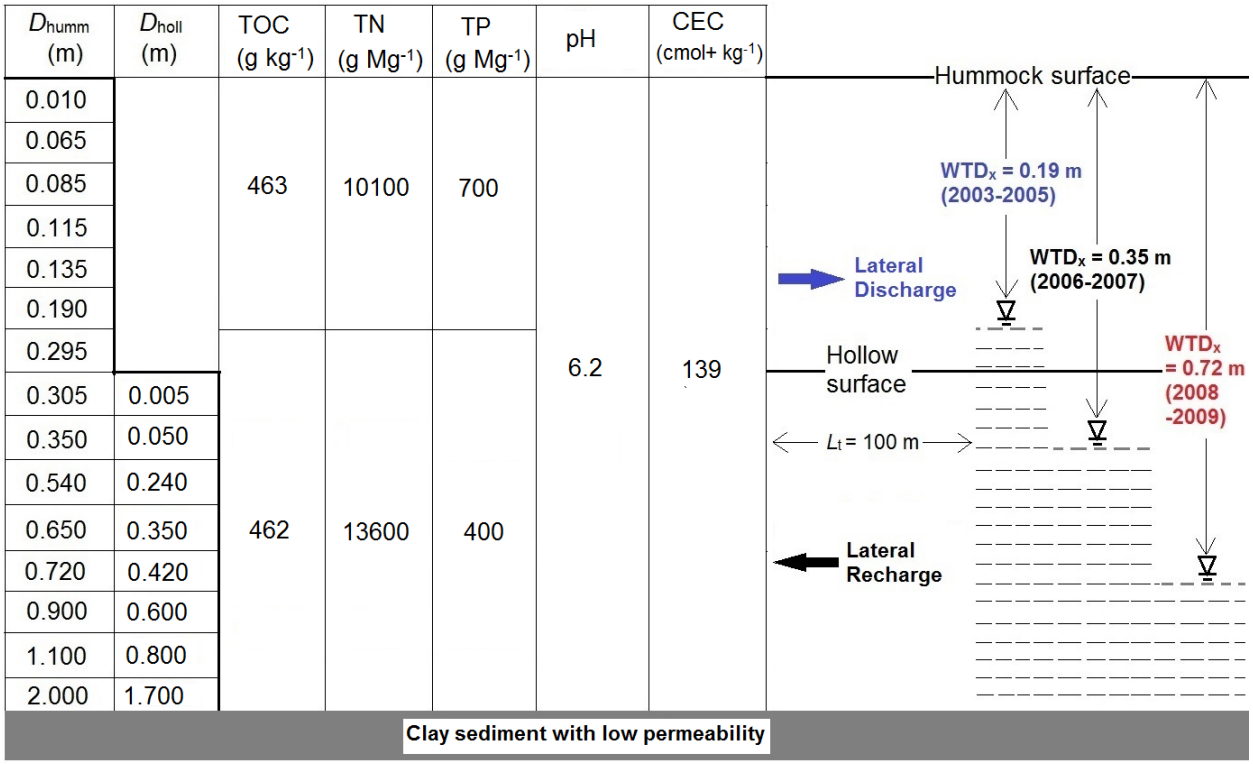

Fig. 2.

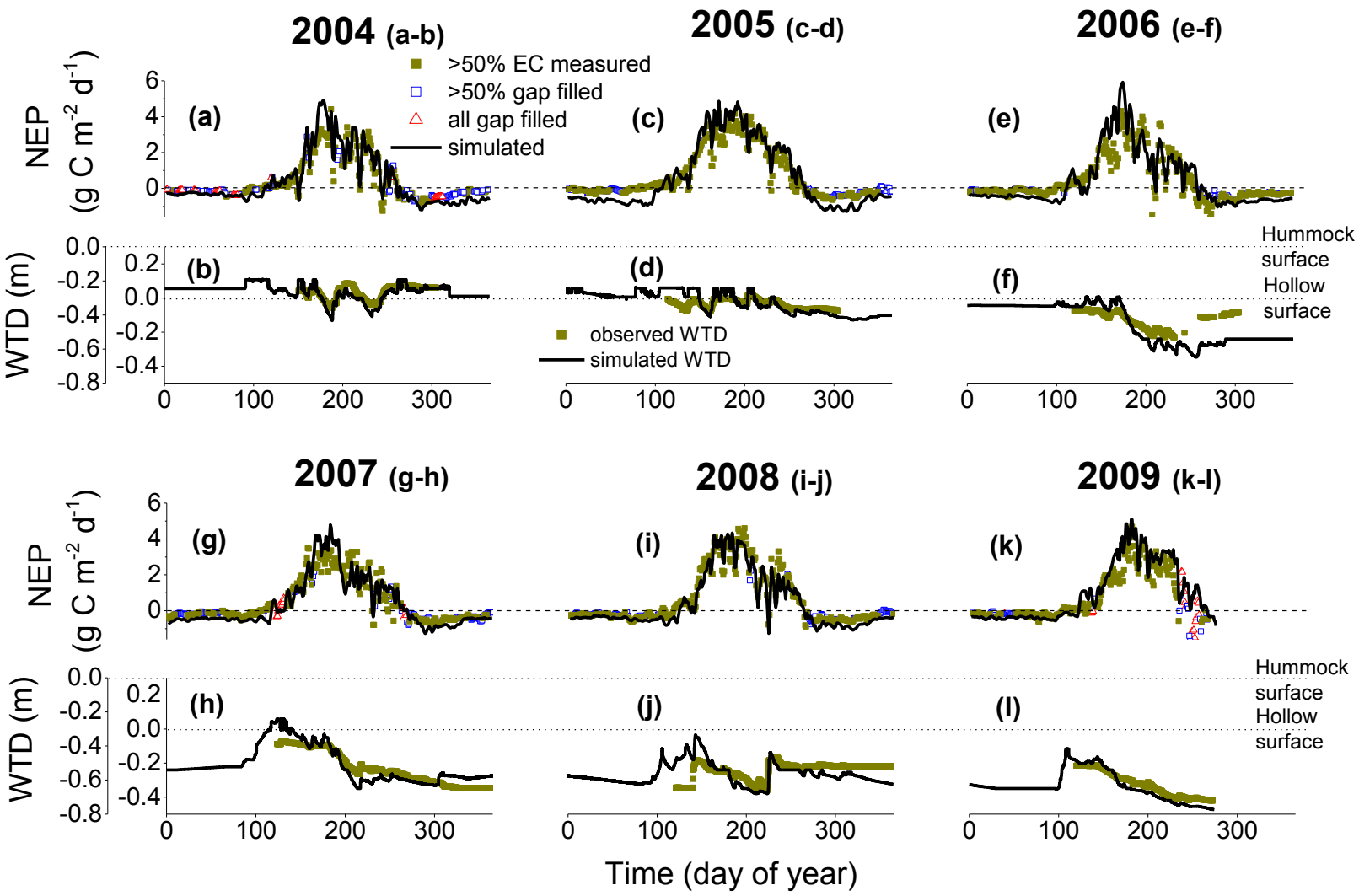

1253

1254 **Fig. 3.**

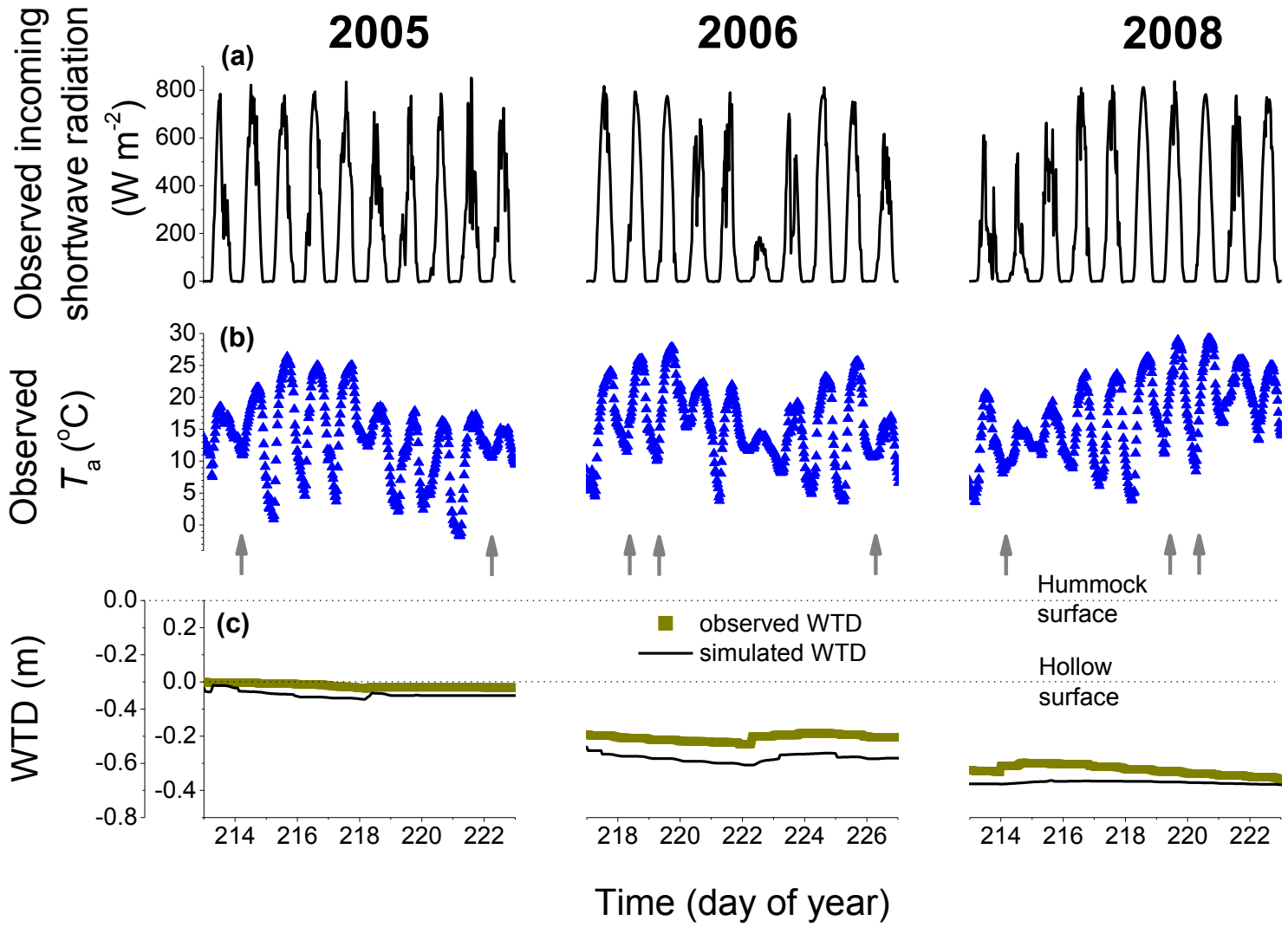

1255

1256 **Fig. 4.**

1257

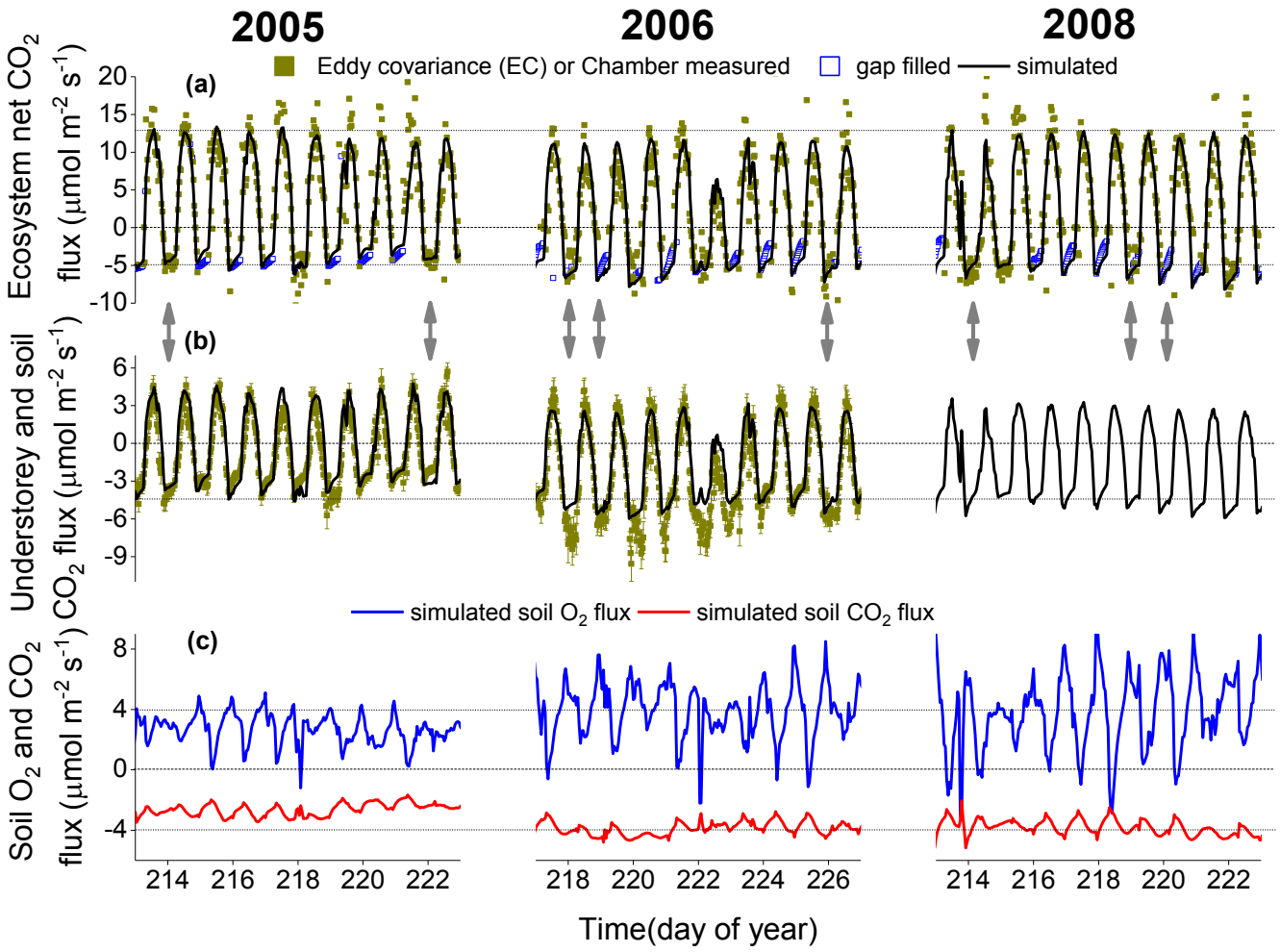

1258

1259 **Fig. 5.**

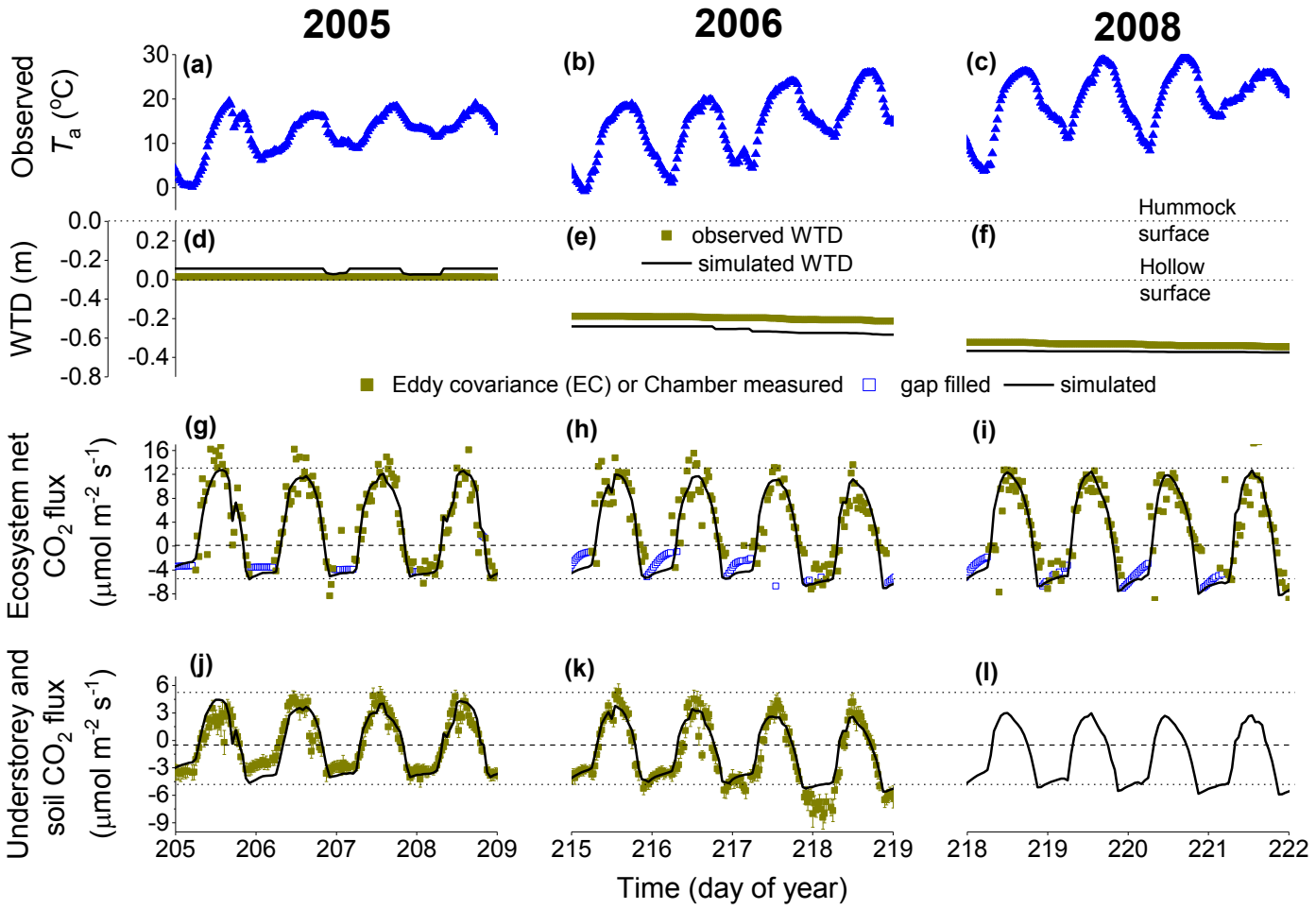
2005
2006
2008
(a)
(b)
(c)
Observed T_a (°C)
(d)
(e)
(f)
WTD (m)
observed WTD
simulated WTD
Hummock surface
Hollow surface
Eddy covariance (EC) or Chamber measured
gap filled
simulated
(g)
(h)
(i)
Ecosystem net CO_2 flux (μmol m^{-2} s^{-1})
(j)
(k)
(l)
Understorey and soil CO_2 flux (μmol m^{-2} s^{-1})
Time (day of year)

Fig. 6.

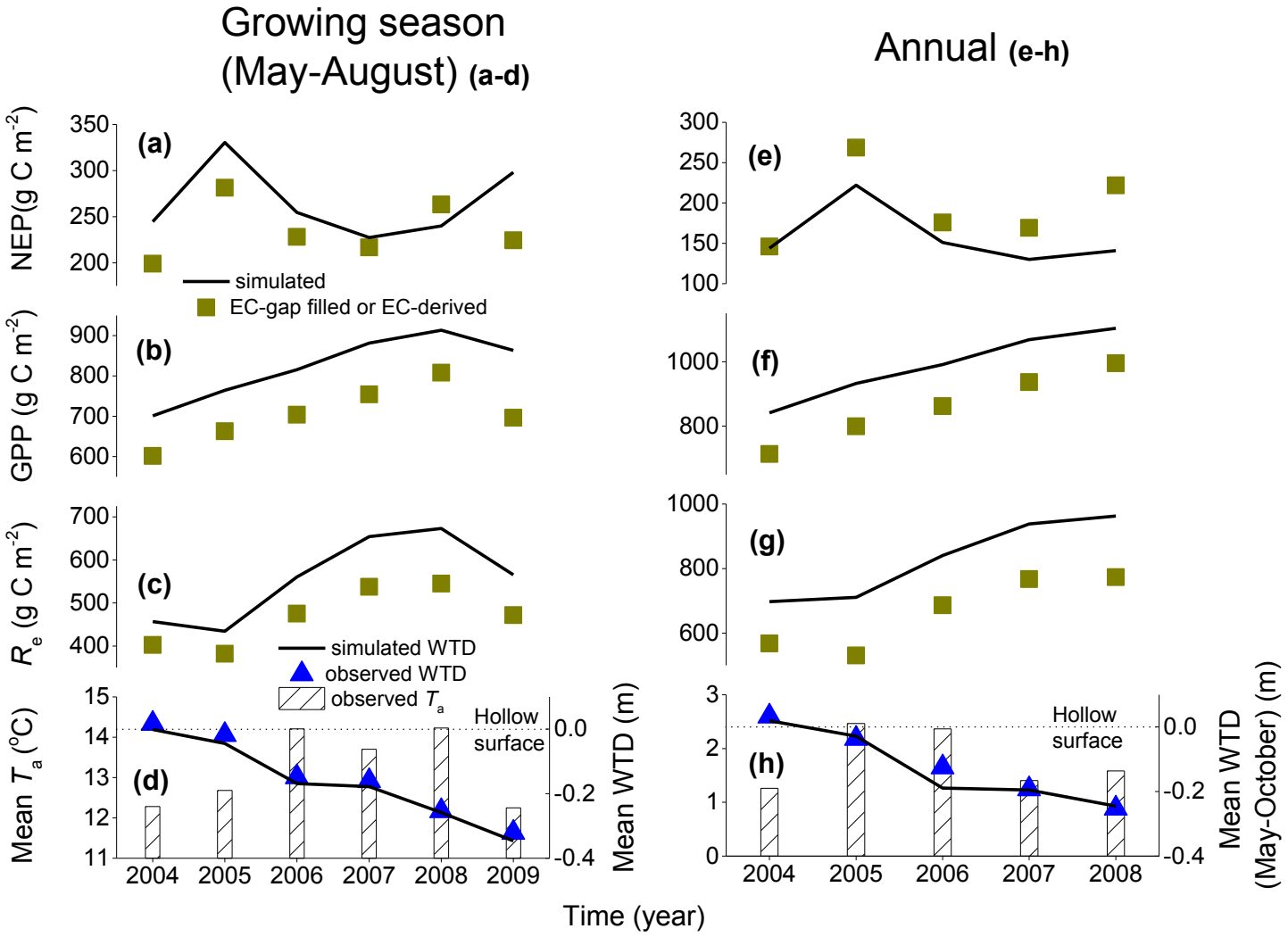

1263

1264 **Fig. 7.**

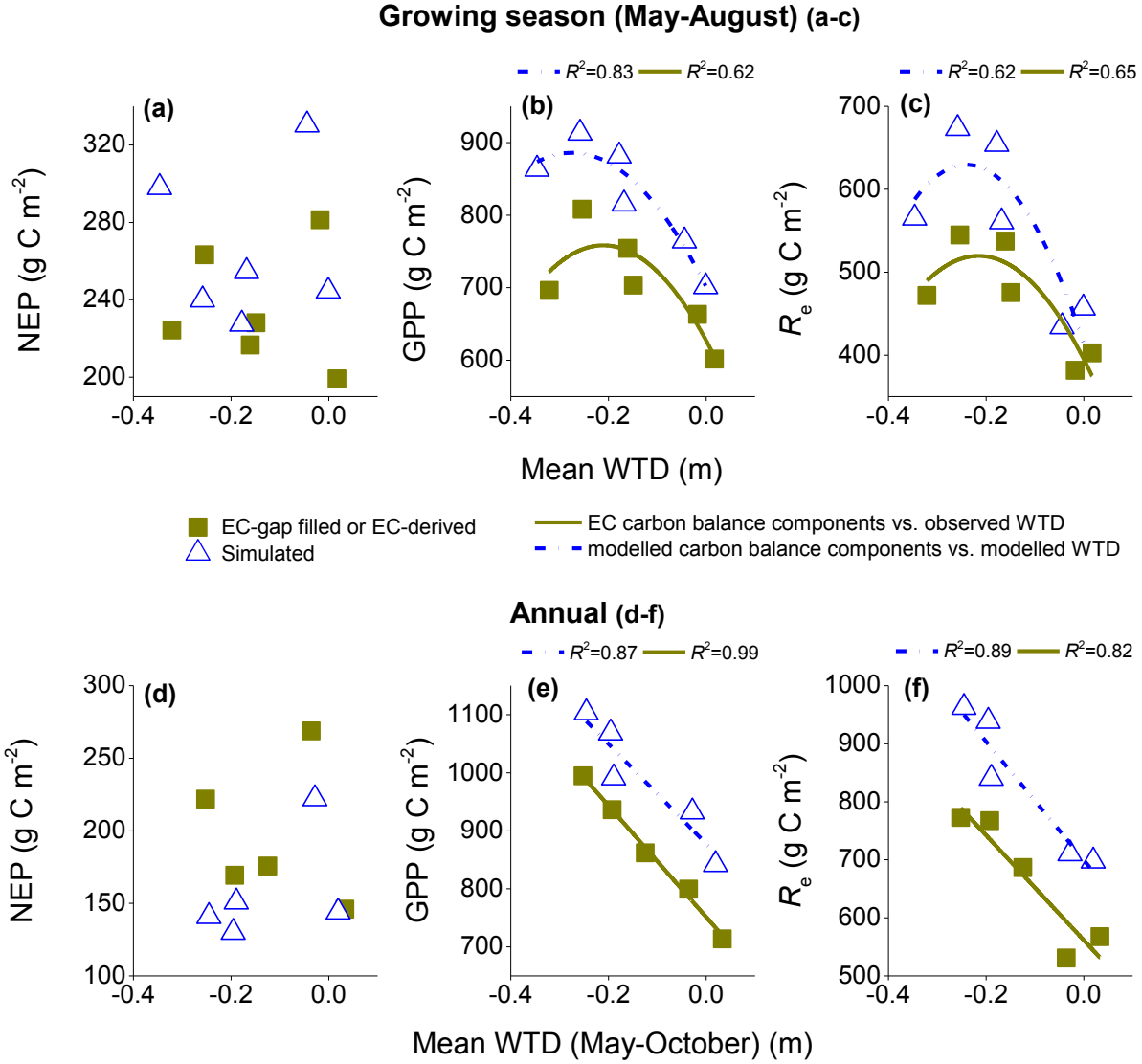

1265

1266 **Fig. 8.**

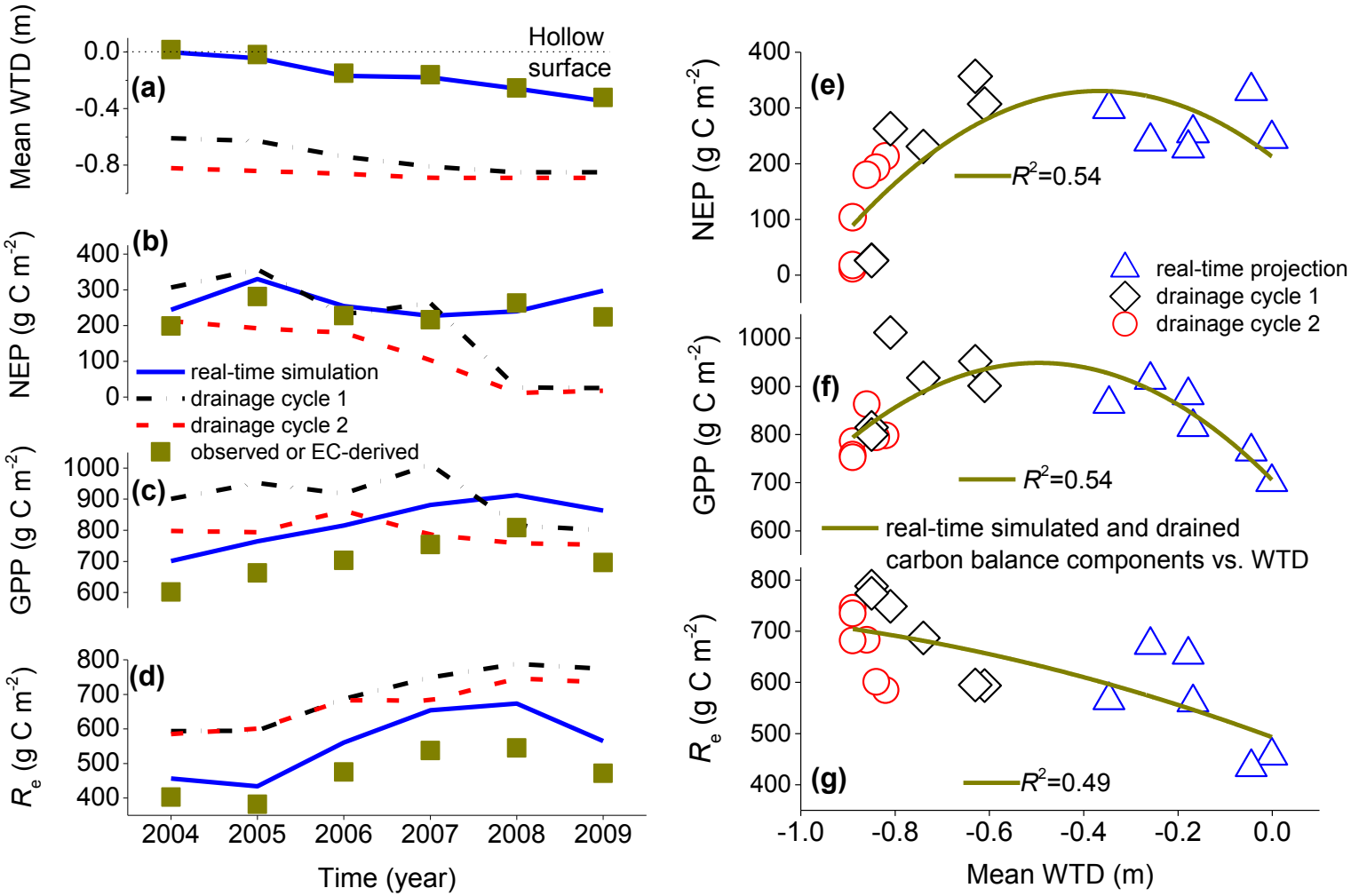

1267

1268 **Fig. 9.**

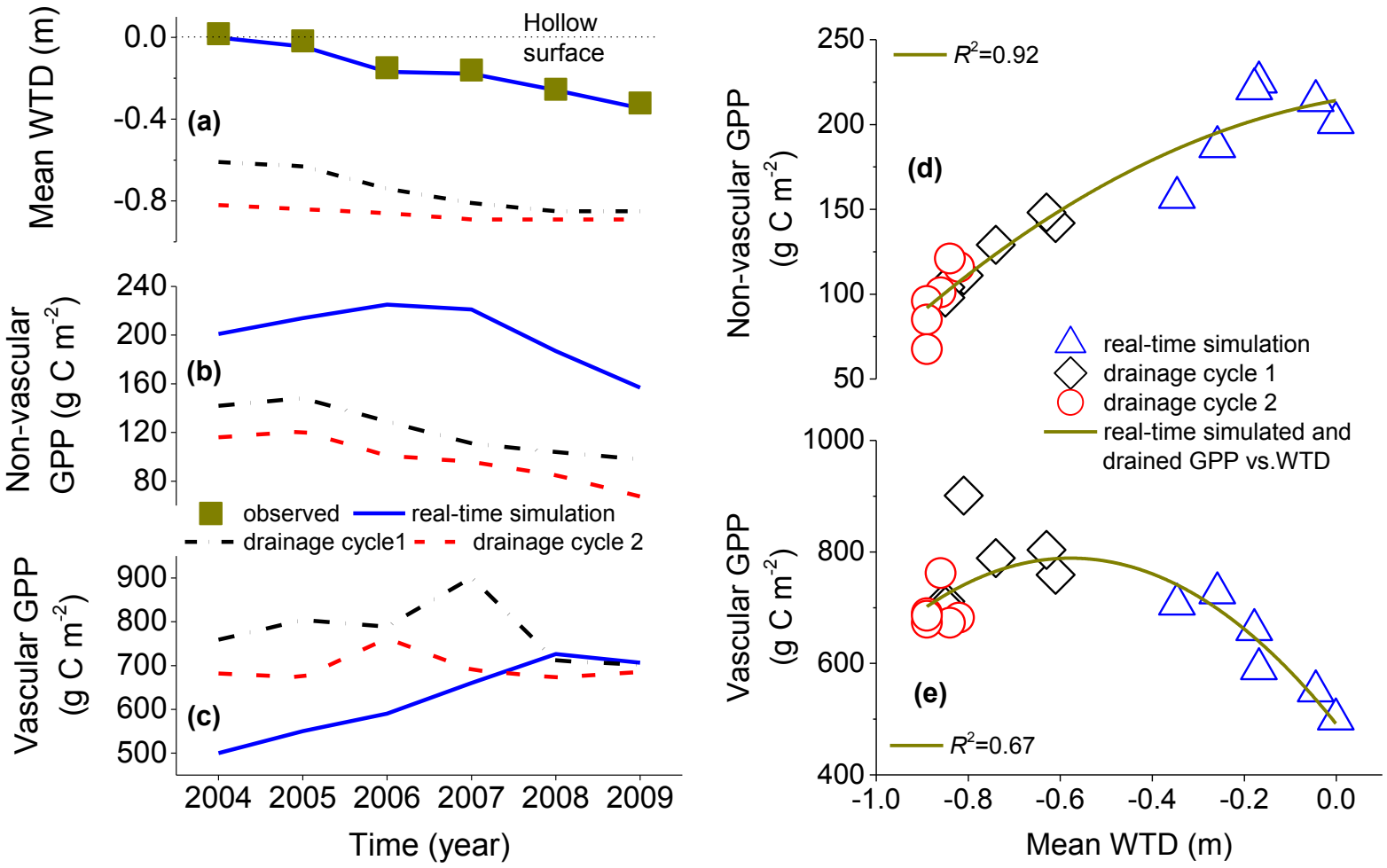

1269

1270 **Fig. 10.**

Table 1. Statistics from regressions between hourly modelled and measured net CO_2 fluxes from 2004-2009 at a Western Canadian fen peatland

(a) Regressions of modelled vs. EC measured (recorded at $u^* > 0.15$ m s^{-1}) net ecosystem CO_2 fluxes over whole years of 2004-2008[a]

Year	Total annual precipitation (mm)	*n*	*a*	*b*	R^2	RMSE (μmol m^{-2} s^{-1})	RMSRE (μmol m^{-2} s^{-1})
2004	553	5034	0.08	1.10	0.81	1.58	1.92
2005	387	5953	0.07	1.03	0.82	1.68	1.99
2006	465	6012	0.07	1.08	0.79	1.68	1.98
2007	431	5385	0.06	0.99	0.79	1.83	2.09
2008	494	5843	-0.01	0.98	0.84	1.63	2.02

(b) Regressions of modelled vs. EC measured (recorded at $u^* > 0.15$ m s^{-1}) net ecosystem CO_2 fluxes over growing seasons (May-August) of 2004-2009

Year	Total growing season precipitation (mm)	*n*	*a*	*b*	R^2	RMSE (μmol m^{-2} s^{-1})	RMSRE (μmol m^{-2} s^{-1})
2004	287	2043	0.55	1.05	0.78	2.27	2.55
2005	276	2200	0.82	0.98	0.79	2.50	2.74
2006	253	2107	0.48	1.06	0.78	2.36	2.76
2007	237	1822	0.65	0.93	0.75	2.91	3.06
2008	276	2070	0.32	0.96	0.82	2.45	2.85
2009	138	1870	0.76	1.01	0.81	2.27	2.83

(c) Regressions of modelled vs. measured chamber net CO_2 fluxes (understorey vegetation and soil CO_2 fluxes) over ice free periods (May-October) of 2005-2006

Year	Mean May-October WTD (m)	*n*	*a*	*b*	R^2	RMSE	RMSRE

							(μmol m^{-2} s^{-1})	(μmol m^{-2} s^{-1})
	Measured	Modelled						
2005	0.34	0.33	3285	0.43	1.05	0.68	1.19	2.38
2006	0.42	0.48	3855	0.31	0.85	0.71	1.44	3.25

WTD = water table depth below the hummock surface; (*a, b*) from simple linear regressions of modelled on measured, and R^2 = coefficient of determination; RMSE = root mean square for errors from simple linear regressions of measured on simulated; RMSRE= root mean square for random errors in measurements from simple linear regressions of simulated on measured. RMSRE for eddy covariance (EC) measurements were calculated by inputting EC CO_2 fluxes recorded at u^* (friction velocity) > 0.15 m s^{-1} into algorithms for estimation of random errors due to EC CO_2 measurements developed for forests by Richardson et al. (2006).

[a] whole year modelled vs. EC net CO_2 flux regression for 2009 could not be done due to the lack of flux measurements from September to December in that year.

Table 2. Effects of water table depth (WTD) drawdown on components of ecosystem carbon and nutrient cycles of a Western Canadian fen peatland

		Modelled	Eddy covariance-derived/biometrically measured at the site [a]	Values from other studies in similar peatlands
Rate of increase in R_e with each 0.1 m of WTD drawdown		0.26 μmol CO_2 m^{-2} s^{-1}	0.16 μmol CO_2 m^{-2} s^{-1}	(1) ~0.3 μmol CO_2 m^{-2} s^{-1} [b] (2) ~0.33 μmol CO_2 m^{-2} s^{-1} [c]
Rate of increase in GPP with each 0.1 m of WTD drawdown		0.39 μmol CO_2 m^{-2} s^{-1}	0.22 μmol CO_2 m^{-2} s^{-1}	(1) ~0.28 μmol CO_2 m^{-2} s^{-1} [b] (2) ~0.44 μmol CO_2 m^{-2} s^{-1} [c]
Leaf nitrogen concentration (July 2004)	Black Spruce	14 g N kg^{-1} C	12 g N kg^{-1} C	
	Tamarack	32 g N kg^{-1} C	33 g N kg^{-1} C	
	Dwarf Birch	37 g N kg^{-1} C	41 g N kg^{-1} C	
Leaf nitrogen (N) to phosphorus (P) ratio (July 2004)	Black Spruce	6.6:1	7.1:1	
	Tamarack	5.2:1	6.3:1	

	Dwarf Birch	4.8:1	
Increase in foliar nitrogen concentrations with WTD drawdown	Black Spruce	from 14 to 17 g N kg^{-1} C with a WTD drawdown from ~0.25 to ~0.65 m below the hummock surface over the growing seasons of 2004-2009	(1) from ~21 to ~27 g N kg^{-1} C with a WTD drawdown from 0.24 to 0.7 m below peat surface [d] (2) from ~19 to ~21 g N kg^{-1} C for a WTD drawdown by ~0.45 m [e]
	Tamarack	from 32 to 37 g N kg^{-1} C with a WTD drawdown from ~0.25 to ~0.65 m below the hummock surface over the growing seasons of 2004-2009	(1) from ~41 to ~66 g N kg^{-1} C for a WTD drawdown from 0.24 to 0.7 m below peat surface [d] (2) from ~36 to ~42 for a WTD drawdown by ~0.45 m [e]
	Dwarf Birch	from 37 to 45 g N kg^{-1} C with a WTD drawdown from ~0.25 to ~0.65 m below the hummock surface over the growing seasons of 2004-2009	
Increase in maximum rooting depth with WTD drawdown	Black spruce	from 0.35 to 0.65 m below the hummock surface with a WTD drawdown from ~0.25 to ~0.65 m over the growing seasons of 2004-2009	from 0.1 to 0.6 m below peat surface with a WTD drawdown from 0.1 to 0.7 m below hummock surface [f]
	Tamarack	from 0.35 to 0.65 m below the hummock surface with a WTD drawdown from ~0.25 to ~0.65 m	from 0.2 to 0.6 m below peat surface with a WTD drawdown

	over the growing seasons of 2004-2009	from 0.1 to 0.6 m below hummock surface [f]

GPP=gross primary productivity; R_e = ecosystem respiration; [a] Syed et al. (2006), Flanagan and Syed (2011); [b] Peichl et al. (2012) for a Swedish fen; [c] Ballantyne et al. (2014) for a Michigan fen peatland complex that has similar peat and plant functional types as our study site; [d] Choi et al. (2007) for a central Alberta fen peatland located ~350 km to the southwest of the study site; [e] Macdonald and Lieffers (1990) for a northern Alberta fen peatland located ~250 km to the northwest of the study site; [f] Lieffers and Rothwell (1987) for a northern Alberta fen peatland located ~250 km to the northwest of the study site